Paradise Lost.
John Milton, c. 1667.

CHAPTER 15

The Buoyancy Driven Circulation

OUR GOAL in this chapter and the next is to gain a rudimentary understanding of the three-dimensional dynamics and structure of the ocean circulation. In this chapter we focus on the *meridional overturning* and the associated *abyssal* circulation of the ocean, treating them as if they were solely driven by buoyancy forces, and in chapter 16 we look at the combined effects of wind and buoyancy forcing.

The meridional overturning circulation (MOC) is so-called because it is associated with sinking at high latitudes and upwelling elsewhere, although as we shall see even such a seemingly simple matter as this is not wholly settled. The circulation is also sometimes known as the 'thermohaline' circulation, reflecting a belief that it is driven by gradients in temperature and salinity, but because other mechanisms are also important that name is not appropriate as a general descriptor. In fact, the theory explaining the MOC is not in as satisfactory a state as it is for the quasi-horizontal wind-driven circulation discussed in chapter 14. In the theory of the wind-driven circulation, a rational series of approximations from the governing Navier-Stokes equations leads to a sequence of simple models (e.g., the homogeneous models of the wind-driven circulation, layered quasi-geostrophic models, etc.) whose foundations are thus reasonably secure, whose shortcomings are understood, and whose behaviour can be fairly completely analyzed. Attempts to proceed in a similar fashion with overturning circulation have been less successful; the reason is that the approximations required in order that a tractable conceptual model be constructed are unavoidably severe and, from a fluid-dynamicist's perspective, unjustifiable. Thus, although the large-scale overturning flow is well-described by the planetary geostrophic equations whose complexity is similar to that of the quasi-geostrophic equations, there is no rational simplification of these that leads to a model that is both as simple and informative as the homogeneous Stommel model of the quasi-horizontal, wind-driven circulation. Nevertheless, progress *has* been

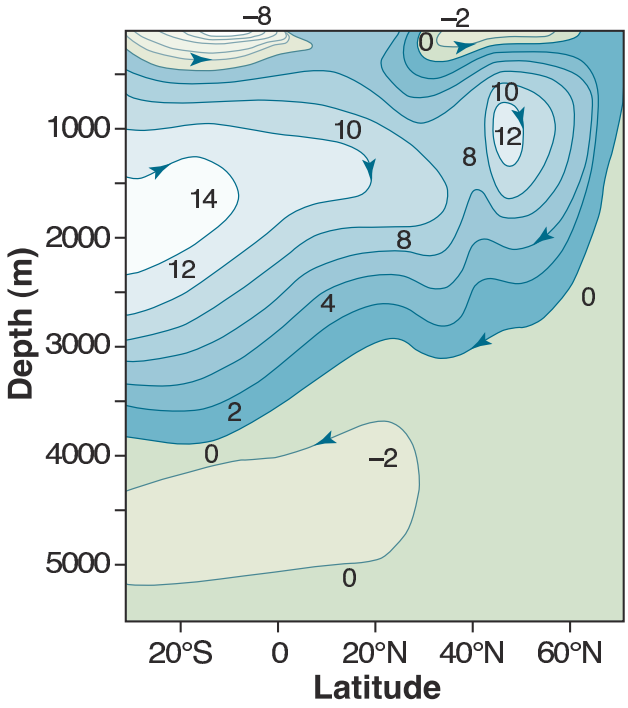

Figure 15.1 The mean meridional overturning circulation in the North Atlantic, obtained with a combination of observations and a model. The contours are the streamfunction of the zonally averaged meridional flow. The units are Sverdrups, and the circulation is mostly clockwise, with sinking at high latitudes.[2]

made, both numerically and through the use of very simple models, and in this chapter we concentrate on the foundations underlying these.

15.1 A BRIEF OBSERVATIONAL OVERVIEW

That there *is* a deep circulation has been known for a long time, largely from observations of tracers such as temperature, salinity and constituents such as dissolved oxygen and silica.[1] We can also take advantage of numerical models that are able to assimilate hydrographic and other observations and produce an estimate of the overturning circulation that is consistent with both the observations and the equations of motion, as illustrated in Fig. 15.1.

Associated with the overturning circulation is a stratification that has a quite distinctiv structure, as illustrated in Fig. 15.2. Most of the stratification is evidently concentrated in the upper kilometre or so of the ocean, with a relatively (although not completely) unstratified abyss full of dense water that has originated from high latitudes — the isopycnals shown in Fig. **??** all outcrop (i.e., intersect the surface) in the North Atlantic subpolar gyre and/or in the Antarctic Cicumpolar Current (ACC). The region of high stratification near the surface is known as the *thermocline* ('thermo' for temperature, 'cline' for changing); it is effectively synonymous with the *pycnocline* (for changing density), although the latter could exist without the former if there were a *halocline*, in which salinity changed rapidly. What is the cause of this circulation and the associated stratification?

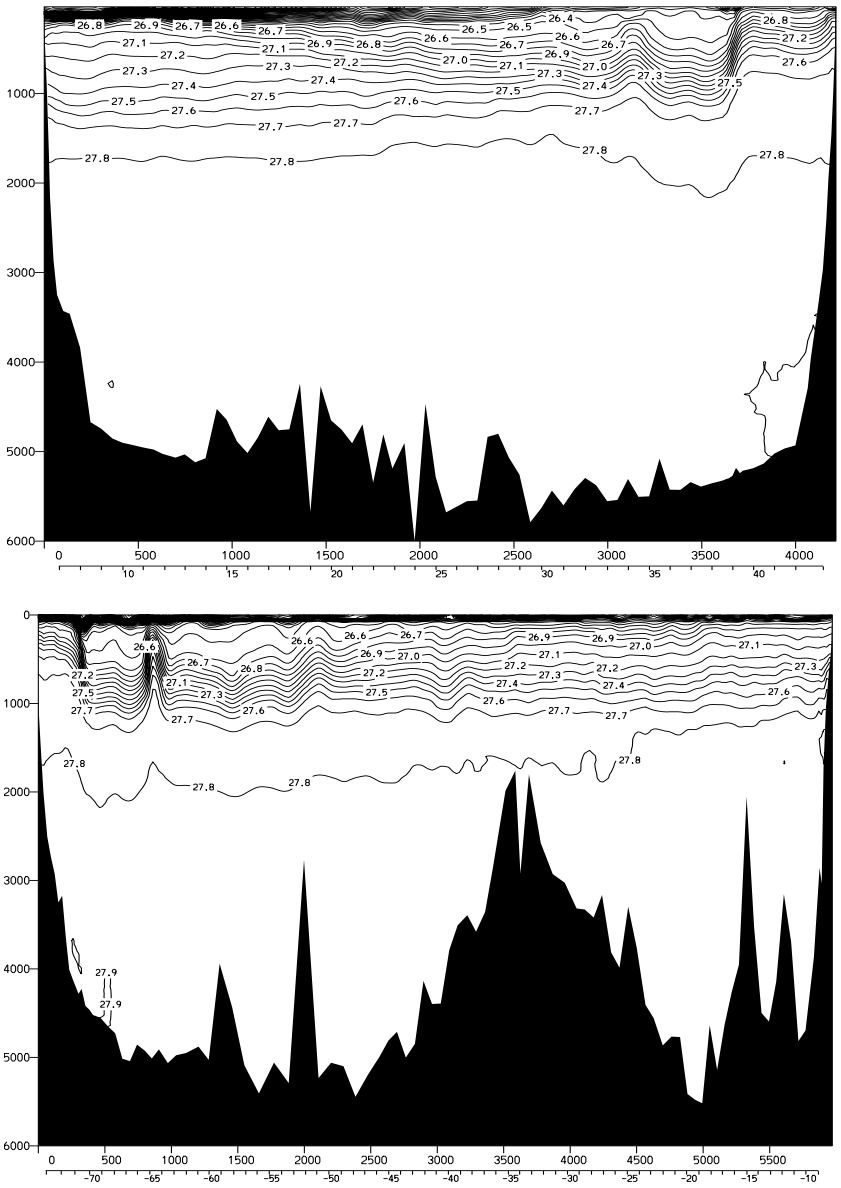

Fig. 15.2 Sections of potential density (σ_θ) in the North Atlantic: Upper panel: meridional section at 53°W, from 5°N to 45°N, across the subtropical gyre. Lower panel: zonal section at 36°N, from about 75°W to 10°W. The region of rapid change of density (and temperature) is concentrated in the upper kilometer, in the *main thermocline,* below which the ocean has a much more uniform density. A front is associated with the western boundary current and its departure from the coast near 40°N. In the upper northwestern region of subtropical thermocline there is a region of low stratification known as MODE water: isopycnals above this outcrop in the subtropical gyre and are 'ventilated'; isopycnals below the MODE water outcrop in the subpolar gyre.[3]

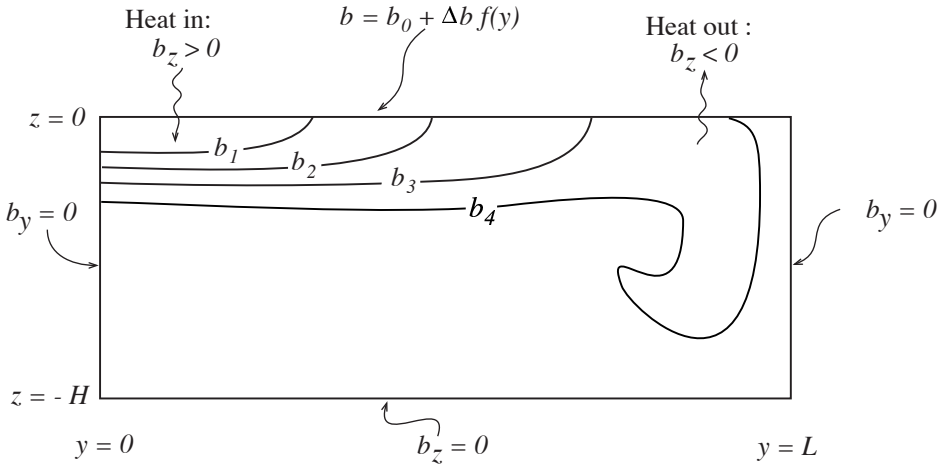

Fig. 15.3 A schema of 'sideways convection'. The y-axis represents latitude and the z-axis represents depth. The fluid is differentially heated and cooled along its top surface, whereas all the other walls are insulating. The result is, typically, a small region of convective instability and sinking near the coldest boundary, with generally upwards motion elsewhere.[4]

15.2 SIDEWAYS CONVECTION

Perhaps the simplest and most obvious fluid dynamical model of the overturning circulation is that of *sideways* or *horizontal convection.* The physical situation is sketched in Fig. 15.3. A fluid (two- or three-dimensional) is held in a container that is insulated on all its sides and bottom, but its upper surface is non-uniformly heated and cooled. In the purest fluid dynamical problem the heat enters the fluid solely by conduction at the upper surface, and one may suppose that here the temperature is imposed. Thus, for a simple Boussinesq fluid the equations of motion are

$$\frac{\mathrm{D}\boldsymbol{v}}{\mathrm{D}t} + \boldsymbol{f} \times \boldsymbol{v} = -\nabla\phi + b\mathbf{k} + \nu\nabla^2\boldsymbol{v}, \tag{15.1a}$$

$$\frac{\mathrm{D}b}{\mathrm{D}t} = \kappa\nabla^2 b, \tag{15.1b}$$

$$\nabla \cdot \boldsymbol{v} = 0, \tag{15.1c}$$

with boundary conditions

$$b(x, y, 0, t) = f(x, y), \tag{15.2a}$$

where $f(x, y)$ is a specified field, and $\partial_n b = 0$ on the other boundaries, meaning that the derivative normal to the boundary, and so the buoyancy flux, is zero. An alternative upper boundary condition is to impose a flux condition whereby

$$\kappa\frac{\partial}{\partial z}b(x, y, 0, t) = g(x, y), \tag{15.2b}$$

where $g(x, y)$ is given. The oceanographic relevance of and (15.2) should be clear: the ocean is heated and cooled from above, and although the thermal forcing in the real

ocean may differ in detail (being in part a radiative flux, and in part a sensible and latent heat transfer from the atmosphere), (15.2) is a useful idealization. In some numerical models of the ocean, the heat input at the top is parameterized by way of a relaxation to some specified temperature. This is a form of flux condition in which

$$\text{Flux} = \kappa \frac{\partial b}{\partial z} = C(b^* - b), \tag{15.3}$$

and C is an empirical constant.[5] Although this may be a little more realistic than (15.2a) it will not affect the arguments below.

15.2.1 Two-dimensional convection

We may usefully restrict attention to the two-dimensional problem, in latitude and height. The two-dimensional flow may then loosely be thought of as representing the statistically steady zonally averaged flow of the ocean, valid only for large spatial scales. The zonally-averaged zonal flow is then small, and concomitantly so is the Coriolis force. The incompressibility of the flow then allows one to define a streamfunction such that

$$v = -\frac{\partial \psi}{\partial z}, \quad w = \frac{\partial \psi}{\partial y}, \qquad \zeta = \nabla_x^2 \psi = \left(\frac{\partial^2 \psi}{\partial y^2} + \frac{\partial^2 \psi}{\partial z^2} \right) \tag{15.4}$$

where ζ is the vorticity in the meridional plane. We will neglect the subscript x on the Laplacian operator where there is no ambiguity. Taking the curl of Boussinesq equations of motion (15.1) then gives

$$\frac{\partial \nabla^2 \psi}{\partial t} + J(\psi, \nabla^2 \psi) = \frac{\partial b}{\partial y} + \nu \nabla^4 \psi \tag{15.5a}$$

$$\frac{\partial b}{\partial t} + J(\psi, b) = \kappa \nabla^2 b \tag{15.5b}$$

where $J(a,b) \equiv (\partial_y a)(\partial_z b) - (\partial_z a)(\partial_y b)$.

Nondimensionalization and scaling

We non-dimensionalize (15.5) by formally setting

$$b = \Delta b\, \hat{b}, \qquad \psi = \Psi \hat{\psi}, \qquad x = L\hat{x}, \qquad z = H\hat{z}, \qquad t = \frac{LH}{\Psi}\hat{t}, \tag{15.6}$$

where the hatted variables are non-dimensional, Δb is the temperature difference across the surface, L is the horizontal size of the domain, and Ψ, and ultimately the vertical scale H, are to be determined. Substituting into (15.6) gives

$$\frac{\partial \widehat{\nabla}^2 \hat{\psi}}{\partial \hat{t}} + J(\hat{\psi}, \nabla^2 \hat{\psi}) = \frac{H^3 \Delta b}{\Psi^2} \frac{\partial \hat{b}}{\partial \hat{y}} + \frac{\nu L}{H} \widehat{\nabla}^4 \hat{\psi} \tag{15.7a}$$

$$\frac{\partial \hat{b}}{\partial \hat{t}} + J(\hat{\psi}, \hat{b}) = \frac{\kappa L}{\Psi H} \widehat{\nabla}^2 \hat{b} \tag{15.7b}$$

where $\widehat{\nabla}^2 = (H/L)^2\partial^2/\partial\hat{y}^2 + \partial^2/\partial\hat{z}^2$ and the Jacobian operator is also appropriately non-dimensional. If we now use (15.7b) to choose Ψ as

$$\Psi = \frac{\kappa L}{H} \tag{15.8}$$

so that $t = H^2\hat{t}/\kappa$, then (15.6) become

$$\frac{\partial\widehat{\nabla}^2\hat{\psi}}{\partial\hat{t}} + J(\hat{\psi}, \nabla^2\hat{\psi}) = Ra\sigma\alpha^5\frac{\partial\hat{b}}{\partial\hat{y}} + \sigma\widehat{\nabla}^4\hat{\psi} \tag{15.9}$$

$$\frac{\partial\hat{b}}{\partial\hat{t}} + J(\hat{\psi}, \hat{b}) = \widehat{\nabla}^2\hat{b} \tag{15.10}$$

and the three non-dimensional parameters that govern the behaviour of the system are

$$Ra = \left(\frac{\Delta b L^3}{\nu\kappa}\right), \qquad \text{(the Rayleigh number)}, \tag{15.11a}$$

$$\sigma = \frac{\nu}{\kappa}, \qquad \text{(the Prandtl number)}, \tag{15.11b}$$

$$\alpha = \frac{H}{L}, \qquad \text{(the aspect ratio)}. \tag{15.11c}$$

The Rayleigh number is a measure of the strength of the buoyancy forcing relative to the viscous term, and in the ocean it will be very large indeed, perhaps $\sim 10^{24}$ if molecular values are used. (Sometimes H is used instead of L in the Rayleigh number definition; we use L here because it is an external parameter.)

For steady non-turbulent flows (or conceivably statistically steady flows in which ν and κ are an eddy viscosity and an eddy diffusivity) then we can demand that the buoyancy term in (15.9) is $\mathcal{O}(1)$. If it is smaller then the flow is not buoyancy driven, and if it is larger there is nothing to balance it. This can only hold if the vertical scale of the motion appropriately adjusts, and for $\sigma = \mathcal{O}(1)$, this leads to the possible scalings[6]

$$H = L\sigma^{-1/5}Ra^{-1/5}, \qquad \Psi = Ra^{1/5}\sigma^{-4/5}\nu. \tag{15.12a,b}$$

Note that the vertical scale arises as a consequence of the scaling analysis, and the vertical size of the domain plays no direct role. (For $\sigma \gg 1$ we might expect the nonlinear terms to be small and if the buoyancy term balances the viscous term in (15.9) the right-hand sides of (15.12) are multiplied by $\sigma^{1/5}$ and $\sigma^{-1/5}$. For seawater $\sigma \approx 7$ with the molecular values of κ and ν. If small scale turbulence exists, then the eddy viscosity will likely be similar to the eddy diffusivity and $\sigma \approx 1$.)

Numerical experiments (Fig. 15.4 and Fig. 15.5) do provide some support for this scaling, and although the range of Rayleigh numbers that has been achieved is limited a few simple and robust points that have relevance to the real ocean do emerge, namely:

- ⋆ Most of the box fills up with the densest available fluid, with a boundary layer in temperature near the surface required in order to satisfy the top boundary condition. The boundary gets thinner with decreasing diffusivity, consistent with (15.12). This is a diffusive prototype of the oceanic thermocline.

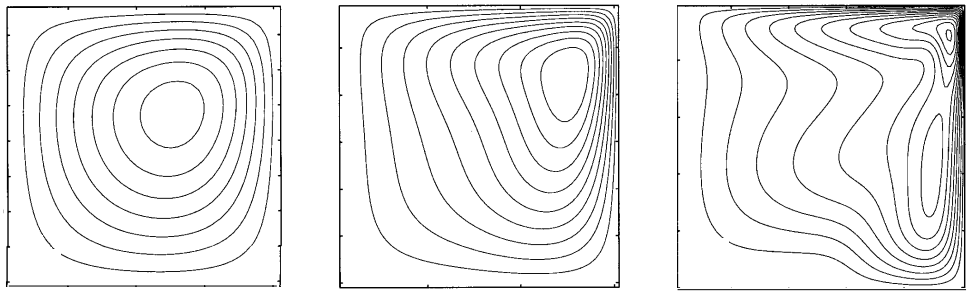

Fig. 15.4 The streamfunction in a numerical simulation of two-dimensional sideways convection. The circulation is clockwise, and the imposed temperature at the top linearly decreases from left to right, and the other walls are insulating. From left to right the Rayleigh numbers are 10^4, 10^6 and 10^8, and the contour interval is 1, 4 and 10 in arbitrary units. The Prandtl number is 10.[7]

- ⋆ The horizontal scale of the overturning circulation is large, being at or near the scale of the box.
- ⋆ The downwelling regions (the regions of active convection) tend to be of smaller horizontal scale than the upwelling regions, especially as the Rayleigh number increases.

Let us now try to explain some of these features in a simple and heuristic way.

15.2.2 Phenomenology of the overturning circulation

No water can be denser (or, more accurately, have a greater potential density) than the densest water at the surface, and if the subsurface water is a little lighter than this the surface water will be convectively unstable and sink in a plume.[8] The plume slowly entrains the warmer water that surrounds it, and then spreads horizontally when it reaches

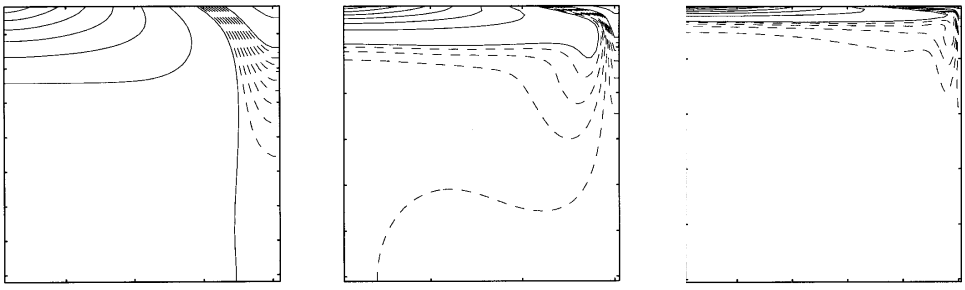

Fig. 15.5 The temperature or buoyancy field corresponding to the streamfunction fields shown in Fig. 15.4. Note an increasingly sharp gradient (a thermocline) near the top as the Rayleigh number increases, and that the bulk of the domain is filled with the densest available fluid.

the bottom or when density becomes similar to that of its surroundings. The presence of water denser than its surroundings creates a pressure gradient, and the ensuing flow will displace any adjacent lighter fluid, and so the domain fills with the densest available fluid. This process is a continous one: the plumes take cold water into the interior, where the water slowly warms by diffusion, and the source of cold water at the surface is continuously replenished. If diffusion is small, the end result is that density of the fluid in the interior will be almost the same as (in fact just slightly less than) that of the densest fluid formed at the surface. (Because diffusion can act only to reduce extrema, no fluid in the interior can be colder than the coldest fluid formed at the surface.) However, the value at the surface is given by the boundary condition $b(x, y, z = 0) = f(x, y)$. Thus, the interior cannot fill all the way to the surface with this cold water and there must be a boundary layer connecting the cold, dense interior with the surface; its thickness δ is given by the height scale of (15.12a), that is

$$\delta \sim L\sigma^{-1/5}Ra^{-1/5} = \left(\frac{L^2\nu\kappa}{\sigma\,\Delta b}\right)^{1/5}. \tag{15.13}$$

Such a strong boundary layer will not necessarily be manifest in the velocity field, however, because the no-normal flow boundary condition on the velocity field is satisfied by setting $\psi = 0$ as a boundary condition to the elliptic problem $\nabla^2\psi = \zeta$, where ζ is the prognostic variable in (15.5a), and this boundary condition has a global effect on the velocity field.

Why is the horizontal scale of the circulation large? The circulation transfers heat meridionally, and it is far more efficient to do this by a single overturning cell than by a multitude of small cells, so although we cannot entirely eliminate the possibility that some instability will produce such small scales of motion, it seems likely the horizontal scale of the mean circulation will be determined by the domain scale. Indeed, at low Rayleigh number we can explicitly calculate an approximate analytic solution to the problem.[9] To do this we define $\mathcal{R} \equiv Ra\alpha^5$ and, with an eye to the nondimensional equations (15.9), we try

$$\widehat{\psi} = \mathcal{R}\psi_1 + \mathcal{R}^2\psi_2 + \mathcal{O}(\mathcal{R}^3), \qquad \widehat{b} = b_0 + \mathcal{R}b_1 + \mathcal{O}(\mathcal{R}^2). \tag{15.14}$$

We also suppose that the aspect ratio is sufficiently small that $\widehat{\nabla}^2 = \partial^2/\partial\widehat{z}^2$. Substituting into (15.9) gives at zeroth order

$$\frac{\partial^2 b_0}{\partial\widehat{z}^2} = 0, \tag{15.15}$$

whence $b_0 = f(x, y)$, which satisfies the boundary conditions at both top and bottom. Proceeding a little further reveals that

$$\frac{\partial^4\psi_1}{\partial\widehat{z}^4} = -\frac{\partial f}{\partial\widehat{y}}, \qquad J(\psi_1, f) = \frac{\partial^2 b_1}{\partial\widehat{z}^2}. \tag{15.16a,b}$$

These equations can be solved, but it is clear without explicitly doing so that $\psi_1(y, z) = (\partial f/\partial y)A(z)$ and $b_1(y, z) = (\partial f/\partial y)^2 B(z)$, and therefore that horizontal form of the

solution is determined by the surface forcing, provided there are no meridional walls that force ψ to zero where $\partial f/\partial y \neq 0$. It is important to realise that *even for large diffusion and viscosity there is no stationary solution:* as soon as we impose a temperature gradient at the top the fluid begins to circulate, a manifestation of the dictum that a baroclinic fluid is a moving fluid, encountered in section 4.2. For higher Rayleigh number the perturbation analysis fails and we must resort to numerical solutions; these (e.g., Fig. 15.4), do show the circulation dominated by a single overturning circulation rather than many small convective cells. We cannot rigorously prove that this will always be the case, but a general energetic argument that shows that the flow cannot in fact break up into a succession of ever smaller cells in a turbulent cascade is given in the next section.

15.3 ENERGETICS OF SIDEWAYS CONVECTION

This section is a slight extension of section 2.4.3, but now with a starring role for diffusion and the boundary conditions. Let us write the equations of motion as

$$\frac{\partial \boldsymbol{v}}{\partial t} + (\boldsymbol{f} + 2\boldsymbol{\omega}) \times \boldsymbol{v} = -\nabla B + b\mathbf{k} + \nu\nabla^2\boldsymbol{v} \tag{15.17a}$$

$$\frac{\partial b}{\partial t} + \nabla \cdot (b\boldsymbol{v}) = Q = J + \kappa\nabla^2 b \tag{15.17b}$$

$$\nabla \cdot \boldsymbol{v} = 0. \tag{15.17c}$$

where B is the Bernoulli function and Q $(= \dot{b})$ is the total heating, with J its non-diffusive component.

15.3.1 The energy budget

To obtain an energy budget we follow the procedure of section 2.4.3. First take the dot product of (15.17a) with $\boldsymbol{v}$ to give

$$\frac{1}{2}\frac{\partial \boldsymbol{v}^2}{\partial t} = -\nabla \cdot (\boldsymbol{v}B) + wb + \nu\boldsymbol{v} \cdot \nabla^2\boldsymbol{v}. \tag{15.18}$$

Integrating over a domain bounded by rigid walls gives the kinetic energy equation

$$\frac{\mathrm{d}}{\mathrm{d}t}\left\langle \frac{1}{2}\boldsymbol{v}^2 \right\rangle = \langle wb \rangle - \varepsilon, \tag{15.19}$$

where angle brackets denote a volume integration and $\varepsilon = -\nu\left\langle \boldsymbol{v} \cdot \nabla^2\boldsymbol{v} \right\rangle = \nu\left\langle \boldsymbol{\omega}^2 \right\rangle$ is the total dissipation of kinetic energy, a positive definite quantity. Thus, in a statistically steady state in which the left-hand side vanishes after time-averaging, the dissipation of kinetic energy is maintained by the buoyancy flux; that is, by a release of potential energy with light fluid ascending and dense fluid descending.

We obtain a potential energy budget by using (15.17b) to write

$$\frac{\mathrm{D}bz}{\mathrm{D}t} = z\frac{\mathrm{D}b}{\mathrm{D}t} + b\frac{\mathrm{D}z}{\mathrm{D}t} = zQ + bw, \tag{15.20}$$

and integrating this over the domain gives the potential energy equation

$$\frac{\mathrm{d}}{\mathrm{d}t}\langle bz\rangle = \langle zQ\rangle + \langle bw\rangle\,. \tag{15.21}$$

Subtracting (15.21) from (15.19) gives the energy equation

$$\frac{\mathrm{d}}{\mathrm{d}t}\left\langle \frac{1}{2}\boldsymbol{v}^2 - bz\right\rangle = -\langle zQ\rangle - \varepsilon. \tag{15.22}$$

15.3.2 The maintenance of a circulation and Sandström's theorem

In a statistically steady state the left-hand side of (15.22) vanishes and the kinetic energy dissipation is balanced by the buoyancy source terms; that is

$$\boxed{\langle zQ\rangle = -\varepsilon}\,. \tag{15.23}$$

The right-hand side is negative definite, and to balance this the heating must be negatively correlated with height. (Note also that $\langle Q\rangle = 0$ if the fluid is not being heated or cooled overall, and the origin of the z-coordinate is immaterial.) Thus, *in order to maintain a circulation in which kinetic energy is dissipated, the heating must occur, on average, at lower levels than the cooling.* Results resembling this are sometimes called, albeit unjustifiably, 'Sandström's theorem'.[10] In the ocean the non-diffusive heating occurs predominantly at the surface, except for the negligible effects of hydrothermal vents. (In fact, the heating at low latitudes occurs at a slightly higher elevation than the cooling at high latitudes, because sea-level is on average a little higher there.) Thus, $\langle Jz\rangle \approx 0$ and a kinetic-energy-dissipating circulation can *only* be maintained, in the absence of mechanical forcing, if the diffusion is non-zero — in that case heat may be diffused from the surface to depth so effectively providing a deep heat source. In the atmosphere, the heating is mostly at the surface and the cooling is higher up, at lower pressure, so that (15.23) does not provide any particularly useful information.

There are a couple of ways to think intuitively about this result. If the heating is below the cooling, then the heated fluid will expand and become buoyant and rise, and a steady circulation between heat source and heat sink can readily be imagined. But if the heating is above the cooling, there is no obvious pathway between source and sink. Another point of view, more appropriate for a compressible fluid, is in terms of work: if the heating is to do work, as it must because this is the source of the energy that is ultimately dissipated, then the heating and concomitant expansion must occur at a higher pressure than the cooling and concomitant compression.

Surface fluxes, diffusion and diffusivity

Suppose that the only heating to the fluid is via diffusion through the upper surface; that is $J = 0$ in (15.17b). We will show that as $\kappa \to 0$ the kinetic energy dissipation does indeed go to zero.[11] Assuming a statistically steady state, integrating (15.17b) horizontally gives

$$\frac{\partial \overline{bw}}{\partial z} = \kappa \frac{\partial^2 \overline{b}}{\partial z^2}, \tag{15.24}$$

where an overbar indicates a horizontal and time average. Integrating this equation up from the bottom (where there is no flux) to a level z gives

$$\overline{wb} - \kappa \overline{b}_z = 0, \tag{15.25}$$

at every level in the fluid. The two terms on the left-hand-side together comprise the total buoyancy flux through the level z, and this vanishes because there is no buoyancy input except at the surface. If we integrate this vertically we have

$$\langle wb \rangle = H^{-1}\kappa \left[\overline{b}(0) - \overline{b}(-H) \right], \tag{15.26}$$

where the angle brackets denote an average over the entire volume. In the limit $\kappa \to 0$, the integrated advective buoyancy flux will vanish, because the term $\overline{b}(0) - \overline{b}(-H)$ remains finite. (This follows because b is conserved on parcels, except for the effects of diffusion which can only act to reduce the value of extrema in the fluid — see also section 10.5.1. Thus, $\overline{b}(0) - \overline{b}(-H)$ can only be as large as the temperature difference at the surface, which is set by the boundary conditions.)

Now consider the kinetic energy budget. Using (15.22) and (15.26) we have in a statistically steady state

$$\varepsilon = H^{-1}\kappa \left[\overline{b}(0) - \overline{b}(-H) \right]. \tag{15.27}$$

The right-hand side is bounded by the maximum difference of b at the surface, so that kinetic energy dissipation goes to zero if the thermal diffusivity goes to zero; that is, $\varepsilon \to 0$ as $\kappa \to 0$ and in particular $\varepsilon < \kappa b_0 / H$ where b_0 is the maximum temperature difference at the surface. We may also consider the limit $(\kappa, \nu) \to 0$ with fixed Prandtl number $\sigma \equiv \nu/\kappa$, and in this limit also the energy dissipation vanishes with κ.

Finally, let us see how the surface temperature is related to the buoyancy flux, for any value of κ. Multiplying (15.17b) by b and integrating over the domain gives the buoyancy variance equation,

$$\frac{1}{2}\frac{\mathrm{d}\langle b^2 \rangle}{\mathrm{d}t} = \kappa \left[\overline{b \frac{\partial b}{\partial z}}\bigg|_{z=0} - \left\langle |\nabla b|^2 \right\rangle \right]. \tag{15.28}$$

We have assumed that the normal derivative of b vanishes on all surfaces except the top one ($z = 0$) and an overbar denotes a horizontal integral. In a statistically steady state,

$$\overline{b \frac{\partial b}{\partial z}}\bigg|_{z=0} = \left\langle |\nabla b|^2 \right\rangle, \tag{15.29}$$

where the overbar and angle brackets now also imply a time average. The right-hand side is positive definite, and thus there must be a positive correlation between b and $\partial b/\partial z$, meaning there is a heat flux into the fluid where it is hot, and a heat flux out of the fluid where it is cold. This result holds no matter whether the upper boundary condition is a condition on b or on $\partial b/\partial z$.

15.3.3 Interpretation

The result encapsulated by (15.27) means that, for a fluid forced only at the surface by buoyancy forcing, as the diffusivity goes to zero so does the energy dissipation. One immediate result, for a fluid of finite viscosity, is that the vorticity in the fluid must go to zero, because $\varepsilon = \nu \left\langle \boldsymbol{\omega}^2 \right\rangle$; this in turn means that the flow cannot be baroclinic, because baroclinicity generates vorticity, even in the presence of viscosity (section 4.2). An even more interesting result follows for a fluid with small viscosity. In turbulent flow, the energy dissipation at high Reynolds number is not a function of the viscosity; if the viscosity is reduced, the cascade of energy to smaller scales merely continues to still smaller scale, generating vorticity at these smaller scales, and the energy dissipation is unaltered, remaining finite even in the limit $\nu \to 0$. In contrast, for a fluid heated and cooled only the upper surface, the energy dissipation *tends to zero* as $\kappa \to 0$, whether or not one is in the high Reynolds number limit. This means that vorticity cannot be generated at the viscous scales by the action of a turbulent cascade, for that would lead to energy dissipation. Effectively, the result prohibits an ocean that is forced only at the surface by a buoyancy flux from having an 'eddy viscosity' that would enable the fluid to efficiently dissipate energy, and if there is no small scale motion producing an eddy viscosity there can be no eddy diffusivity either. This is a rather different picture from that which describes the real ocean, where there is some dissipation of energy in the interior because of breaking gravity waves, and dissipation at the boundary in Ekman layers, and the eddy diffusivity is needed for there to to be a non-negligible buoyancy-driven meridional overturning circulation.

Of course, thermal forcing in the ocean is in part an imposed flux, coming from radiation among other things, and this penetrates below the surface. However, this makes little real physical difference, provided that this forcing remains confined to the upper ocean. If so, then for any level below this forcing we still have the result (15.25), and the final result (15.27) holds, assuming that the range of temperatures produced by the forcing is still finite.

15.3.4 The importance of mechanical forcing

The real ocean *does* have a deep circulation, so something is missing. Suppose we add a mechanical forcing, $\boldsymbol{F}$, to the right-hand-side of (15.17a); this might represent wind forcing at the surface, or tidess. The kinetic energy budget becomes

$$\varepsilon = \langle wb \rangle + \langle \boldsymbol{F} \cdot \boldsymbol{v} \rangle = H^{-1} \kappa [\overline{b}(0) - \overline{b}(-H)] + \langle \boldsymbol{F} \cdot \boldsymbol{v} \rangle \,. \tag{15.30}$$

In this case even for $\kappa = 0$ there is a source of energy and turbulence (i.e., a dissipative circulation) can be maintained. We emphasize that the results of (15.23) and (15.27) do not prohibit there being a thermal circulation, with fluid sinking at high latitudes and rising at low. However, in the absence of any mechanical forcing this circulation must be laminar as $\kappa \to 0$, even at high Rayleigh number, and the flow is not allowed to break in such a way that energy can be dissipated — a very severe constraint that most flows cannot satisfy. The solution most likely adopted by the fluid is for the flow to

become confined to a very thin layer at the surface, with no abyssal motion at all, which is completely unrealistic vis-a-vis the observed ocean.

Now, turbulent motion at small scales provides a mechanism of mixing and so can effectively generate an 'eddy diffusivity' of buoyancy. *Given* such an eddy diffusivity, it is by no means self-evident that wind forcing is subsequently important for the overturning circulation. That is to say, it is useful to think of mechanical forcing as having two distinct effects:

(i) The wind provides a stress on the surface that may directly drive the large-scale circulation, including the overturning circulation. (An explicit example of this is discussed in section 16.5.)

(ii) Both tides and the wind provide a mechanical source of energy to the system that allows the flow to become turbulent and so provides a source for an eddy diffusivity and eddy viscosity.

In either case, we may conclude that presence of mechanical forcing is necessary for there to be an overturning circulation in the world's oceans of the kind observed. In the remainder of this chapter we ignore the first of these effects, and we suppose that the most important effect of the wind is that it provides an eddy diffusivity to the ocean that is much larger than the molecular value; this then allows large volumes of the ocean to become mixed, so allowing a substantial buoyancy-driven overturning circulation (sometimes called a thermohaline circulation). We first consider extremely simple models of this circulation, so-called box models.

15.4 SIMPLE BOX MODELS

Even though they are far simpler than the real ocean, the fluid dynamical models of the previous section are still quite daunting. The analysis that can be performed is either very specific and of little generality, for example the construction of solutions at low Rayleigh number, of it is a very general form, being of the form of scaling or energetic arguments at high Rayleigh number. Models based on the fluid dynamical equations do not easily allow for the construction of explicit solutions in the parameter regime — high Rayleigh and Reynolds numbers — of interest. It is therefore useful to consider an extreme simplification of the overturning circulation, *box models.* These are very simple caricatures of the circulation, constructed by dividing the ocean into a very small number of boxes with simple rules determining the transport of fluid properties between them.[12] The purist may consider this section a diversion away from a consideration of the fluid dynamical properties of the ocean, but such box models have been quite fecund and an evident source of qualitative understanding, and thus find a place in our discussion.

15.4.1 A Two-Box Model

Consider two boxes as illustrated in Fig. 15.6. Each box is well-mixed and has a uniform temperature and salinity, T_1, T_2 and S_1, S_2. The boxes are connected with a capillary tube at the bottom along which the flow is viscous, obeying Stokes' Law. That

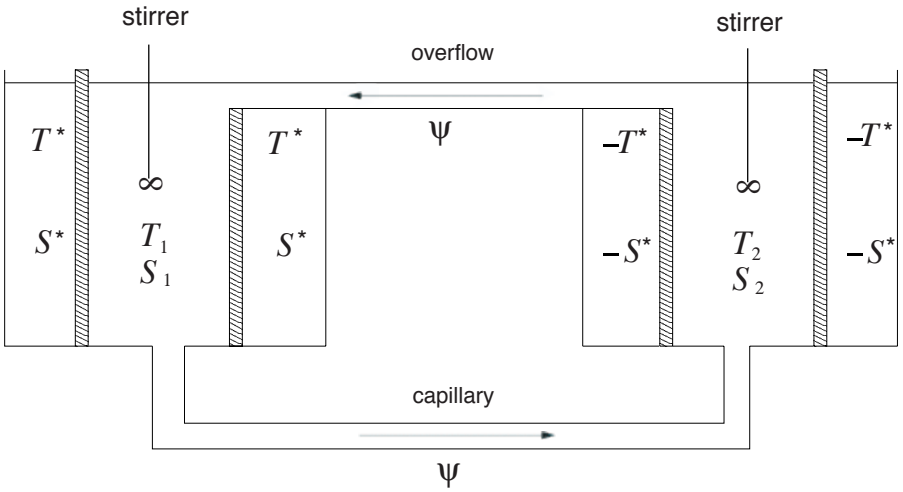

Fig. 15.6 A two-box model of relevance to the overturning circulation of the ocean. The shaded walls are porous, and each box is well-mixed by its stirrer. Temperature and salinity evolve by way of fluid exchange between the boxes via the capillary tube and the overflow, and by way of relaxation with the two infinite reservoirs at $(+T^*, +S^*)$ and $(-T^*, -S^*)$.

is, the flow along the tube is proportional to the pressure gradient which, because the flow is hydrostatic, is proportional the density difference between the two boxes. An overflow at the top keeps the upper surfaces of the two boxes at the same level. Thus, the circulation is given by

$$\Psi = A(\rho_1 - \rho_2), \tag{15.31}$$

where Ψ is proportional to the flow in the pipe, ρ_1 and ρ_2 are the densities of the fluids in the two boxes and A is a constant. The boxes are enclosed by porous walls beyond which are reservoirs of constant temperature and salinity, and we are at liberty to choose the origin of the temperature scale such that the two reservoirs are at $+T^*$ and $-T^*$, and similarly for salinity. Thus, heat and salinity are transferred into and out of the boxes as represented by simple linear laws and we have

$$\begin{aligned} \frac{\mathrm{d}T_1}{\mathrm{d}t} &= c(T^* - T_1) - 2|\Psi|(T_1 - T_2), \quad \frac{\mathrm{d}T_2}{\mathrm{d}t} = c(-T^* - T_2) - 2|\Psi|(T_2 - T_1), \\ \frac{\mathrm{d}S_1}{\mathrm{d}t} &= d(S^* - S_1) - 2|\Psi|(S_1 - S_2), \quad \frac{\mathrm{d}S_2}{\mathrm{d}t} = d(-S^* - S_2) - 2|\Psi|(S_2 - S_1). \end{aligned} \tag{15.32}$$

Note that the advective transfer is independent of the sign the circulation, because it occurs through both the capillary tube and the overflow.

From these equations it is apparent that the sum of the temperatures, $T_1 + T_2$ decays to zero and is uncoupled from the difference, and similarly for salinity. Defining $\widehat{T} =$

$(T_1 - T_2)/(2T^*)$ and $\widehat{S} = (S_1 - S_2)/(2S^*)$ then gives

$$\begin{aligned} \frac{\mathrm{d}\widehat{T}}{\mathrm{d}t} &= c(1-\widehat{T}) - 2|\Psi|\widehat{T} \\ \frac{\mathrm{d}\widehat{S}}{\mathrm{d}t} &= d(1-\widehat{S}) - 2|\Psi|\widehat{S} \end{aligned} \tag{15.33}$$

Using a linear equation of state of the form $\rho = \rho_0(1 - \beta_T T + \beta_S S)$ (where the variables are dimensional) the circulation (15.31) becomes

$$\Psi = 2\rho_0 T^* \beta_T A \left(-\widehat{T} + \frac{\beta_S S^*}{\beta_T T^*} \widehat{S} \right). \tag{15.34}$$

Finally, nondimensionalizing time using $\tau = ct$, the equations of motion become

$$\frac{\mathrm{d}\widehat{T}}{\mathrm{d}\tau} = (1-\widehat{T}) - |\Phi|\widehat{T}, \tag{15.35a}$$

$$\frac{\mathrm{d}\widehat{S}}{\mathrm{d}\tau} = \delta(1-\widehat{S}) - |\Phi|\widehat{S}, \tag{15.35b}$$

$$\Phi = -\gamma(\widehat{T} - \mu\widehat{S}), \tag{15.35c}$$

where the three parameters that determine the behaviour of the system are

$$\gamma = \frac{4\rho_0 T^* \beta_T A}{c}, \qquad \delta = \frac{d}{c}, \qquad \mu = \frac{\beta_S S^*}{\beta_T T^*}. \tag{15.36}$$

The parameter γ measures the overall strength of the forcing in determining the strength of the circulation, and is the ratio of a relaxation to an advective timescale. The parameter δ is the ratio of the reciprocal time constants of temperature and salinity relaxation, and μ is a measure of the ratio of the effect of the salinity and temperature forcings on the density. Salinity transfer will normally be much slower than heat transfer so that $\delta \ll 1$, whereas if salinity and temperature are both to play a role in the dynamics we need $\mu = \mathcal{O}(1)$. We also might expect both advection and relaxation to be important if $\gamma = \mathcal{O}(1)$, and this will depend on the properties of the capillary tube.

Interpretation

The above model describes a potentially real system, one that might be constructed in the laboratory, and one with relevance to aspects of the ocean circulation. One box then represents the entire high-latitude ocean and the other the entire low-latitude ocean, and the capillary tube and the overflow carry the overturning circulation between them. The reservoirs at $\pm T^*$ and $\pm S^*$ represent the atmosphere. Typically, we would choose the low latitudes to be both heated and salted (the latter because of the low rainfall and high evaporation in the subtropics) and the high latitudes to be cooled and freshened by rainfall. Thus, T^* and S^* have the same sign, and they force the circulation in opposite directions. Given the common fluid-dynamical experience that the behaviour of highly-truncated systems often has little resemblance to that of the complete system,

this may only be a cartoon of the ocean circulation. For example, we have restricted the circulation to be of basin scale, and the parameterization of the intensity of the overturning circulation by (15.35c) must be regarded with caution, because it represents a frictionally controlled flow rather than a nearly inviscid geostrophic flow. However, observations and numerical simulations do indicate that the overturning circulation does have a relatively simple vertical and horizontal structure: the circulation in the North Atlantic is similar to that of a single cell, for example, indicating that an appropriate low-order model may be useful.

One might also question the oceanic appropriateness of the linear relaxation terms. For temperature, the bulk ærodynamic formulae often used to parameterize air-sea transport do have a similar form, but the freshening of sea-water by rainfall is more akin to an imposed (negative) flux of salinity, and evaporation is a function of temperature. An alternative might be to impose a salt flux so that

$$\frac{\mathrm{d}}{\mathrm{d}t}(S_1 - S_2) = 2E - 2|\Psi|(S_1 - S_2) \tag{15.37}$$

where E is an imposed, constant, rate of salt exchange with the atmosphere. After nondimensionalization, using E/c to nondimensionalize salt, (15.35b) is replaced by

$$\frac{\mathrm{d}S}{\mathrm{d}\tau} = 1 - |\Phi|S. \tag{15.38}$$

Another aspect of the model that is oceanographically questionable is that it assumes that the water masses can be mixed below the surface. Thus, when water enters one box from the other it immediately mixes with its surroundings. Without the stirrer to ensure this this would not occur and the equations of box model would not represent a real system. In the real ocean, most of the mixing of water masses seems to happen near the surface (in the mixed layer) and near lateral boundaries or possibly regions of steep topography. Elsewhere in the ocean mixing is quite small, and likely far from sufficient to mix a large volume of water in the advective or relaxation times of the box model. We will defer consideration of this and continue with an analysis of the model.

Solutions

Perhaps the most interesting aspect of the set (15.35) is that it exhibits *multiple equilibria;* that is, there are multiple steady solutions with the same parameters. Equilibria occur when the time-derivatives vanish, and the circulation satisfies

$$\Phi = \phi(\Phi) \equiv \gamma\left(\frac{-1}{1+|\Phi|} + \frac{\mu}{1+|\Phi|/\delta}\right). \tag{15.39}$$

A graphical solution of this is obtained as the intercept of the right-hand side with the left-hand side, the latter being a straight line through the origin at an angle of 45°, and this is plotted in Fig. 15.7.

Evidently, for a range of parameters three solutions are possible, whereas for others only one solution exists. Although a fairly complete analysis of the nature of the steady solutions is possible, it is instructive to consider the special case with $\gamma \gg 1$ and

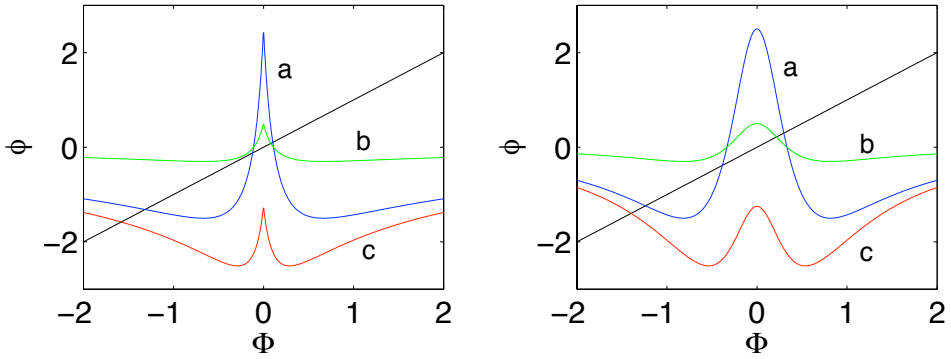

Fig. 15.7 Left panel: Graphical solution of the two-box model. The straight line has unit slope and passes through the origin, and the curved lines plot the function $\phi(\Phi)$ as given by the right-hand-side of (15.39). The intercepts of the two are solutions to the equation. The parameters for the three curves are: a, $\gamma = 5$, $\delta = 1/6$, $\mu = 0.1.5$; b, $\gamma = 1$, $\delta = 1/6$, $\mu = 1.5$; c, $\gamma = 5$, $\delta = 1/6$, $\mu = 0.75$. Right panel: same except with Φ^2 in place of $|\Phi|$ on rhs of (15.39).

$\delta \ll 1$. This corresponds to the situation in which the advective timescale is shorter than the diffusive one and temperature relaxation is much faster than salt relaxation. Two of the solutions are then close to the origin, with $\Phi \ll 1$ and satisfying

$$\Phi = \phi(\Phi) \equiv \gamma \left(-1 + \frac{\mu\delta}{\delta + |\Phi|} \right). \tag{15.40}$$

giving for small $|\Phi|$

$$\Phi \approx \pm[\delta(\mu - 1)]. \tag{15.41}$$

Only the positive solution will be stable, and this solution is driven by the density gradient in salinity; the high salinity of box 1 outweighs (so to speak) the compensating fact that it is also warmer, leading to a flow along the capillary tube from box 1 to box 2. Solving for temperature and salinity we find that $T \approx 1$ (i.e., it is close to its relaxation value and hardly altered by advection), and $S \approx 2 - \mu$ or μ, for $\mu < 2$ and $\mu > 2$ respectively. The saline contribution to density can therefore be larger than that of temperature, and indeed is so for this solution.

The other solution has a circulation far from the origin, and the balance in (15.39) is between the left-hand-side and the first term on the right. In the limiting case we find

$$\Phi \approx -\sqrt{\gamma}. \tag{15.42}$$

This solution has a density gradient dominated by the temperature effect: the temperature difference is $T \approx 1/\sqrt{\gamma}$ whereas the salinity difference is $S \approx \delta/\sqrt{\gamma}$, and thus its effect on density is much smaller.

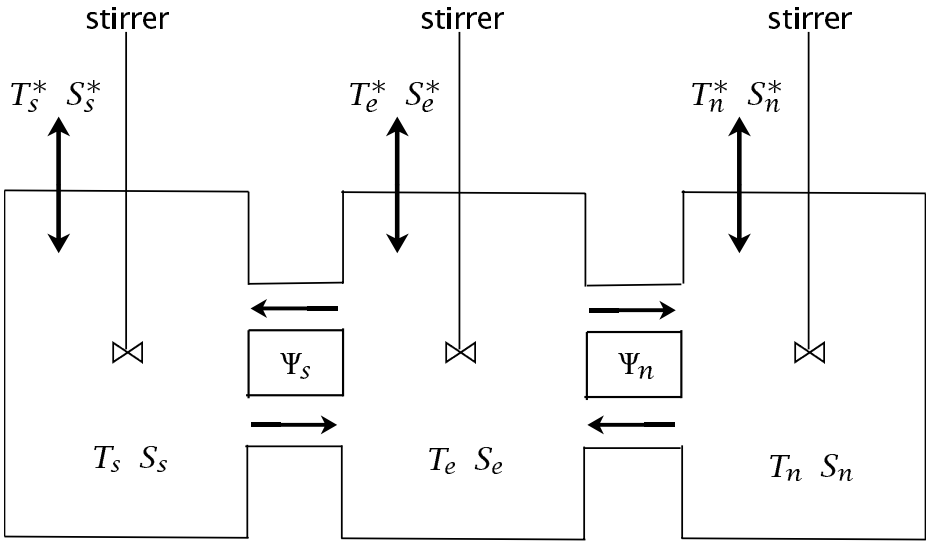

Fig. 15.8 A three-box model. Each box has a constant value of temperature and salinity within it, each exchanges fluid with its neighbour, and in each the temperature and salinity are relaxed back to fixed atmospheric values.

15.4.2 More boxes

More boxes can be added in a variety of ways and, now forgoing an easy relevance to a laboratory apparatus, one such is illustrated in Fig. 15.8. The three boxes represent the mid- and high-latitude northern hemisphere, the mid- and high-latitude southern hemisphere, and the equatorial regions. Each of the three boxes can exchange fluid with its neighbour, and each is also in contact with a reservoir and subject to a relaxation to a fixed value of temperature and salinity, (T_s^*, S_s^*), (T_e^*, S_e^*), (T_n^*, S_n^*). (A variation on this theme allows direct communication between the two poleward boxes.) Then, with obvious notation, we infer the equations of motion:

$$\begin{aligned}
\frac{\mathrm{d}T_s}{\mathrm{d}t} &= c(T_s^* - T_s) - 2|\Psi_s|(T_s - T_e), \qquad \frac{\mathrm{d}T_n}{\mathrm{d}t} = c(T_n^* - T_s) - 2|\Psi_n|(T_n - T_e),\\
\frac{\mathrm{d}T_e}{\mathrm{d}t} &= c(T_e^* - T_e) - |\Psi_s|(T_e - T_s) - |\Psi_n|(T_e - T_n),\\
\frac{\mathrm{d}S_s}{\mathrm{d}t} &= d(S_s^* - S_s) - 2|\Psi_s|(S_s - S_e), \qquad \frac{\mathrm{d}S_n}{\mathrm{d}t} = d(S_n^* - S_s) - 2|\Psi_n|(S_n - S_e),\\
\frac{\mathrm{d}S_e}{\mathrm{d}t} &= d(S_e^* - S_e) - |\Psi_s|(S_e - S_s) - |\Psi_n|, (S_e - S_n),
\end{aligned} \tag{15.43}$$

with flow rates given by the density differences.

$$\Psi_s = A\rho_0[-\beta_T(T_s - T_e) + \beta_S(S_s - S_e)], \quad \Psi_n = A\rho_0[-\beta_T(T_n - T_e) + \beta_S(S_n - S_e)]. \tag{15.44}$$

These equations may be nondimensionalized and reduced to four prognostic equations for the quantities $T_e - T_n$, $T_e - T_s$, $S_e - S_n$, $S_e - S_s$. Not surprisingly, multiple equi-

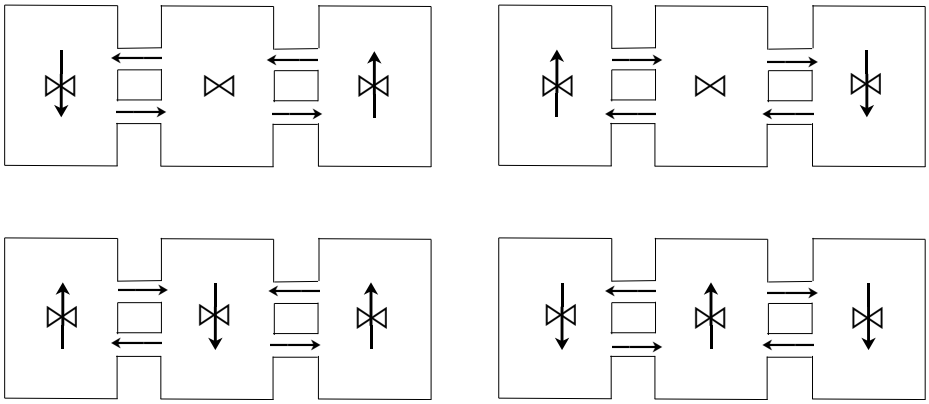

Fig. 15.9 Schematic of four solutions to the three box model with the symmetric forcing $S_s^* = S_n^*$ and $T_n^* = T_s^*$. The two solutions on the top row have an asymmetric, 'pole-to-pole', circulation whereas the solutions on the bottom row are symmetric.[13]

libria can again be found. One particularly interesting aspect is that stable asymmetric solutions arise with symmetric forcing ($T_s^* = T_n^*$, $S_s^* = S_n^*$). These effectively have a pole-to-pole circulation, illustrated in the upper row of Fig. 15.9. Such a circulation can be thought of as the superposition of a thermal circulation in one hemisphere and a salinity-driven circulation in the other.

The box models are useful because they are suggestive of behaviour that might occur in real fluid systems, and because they provide a means of interpreting behaviour that does occur in more complete numerical models, and perhaps in the real world. But without other supporting evidence the solutions found in box models should not be regarded as representing real solutions of the fluid equations for the world's oceans.[14]

15.5 A LABORATORY MODEL OF THE ABYSSAL CIRCULATION

We now return to a more fluid dynamical description of the deep ocean circulation, and consider two simple, closely related, models that are relevant to aspects of the deep circulation. The first, which we consider in this section, is a laboratory model that, although originally envisioned as being a prototype for the deep circulation, is also illustrative of the principles of the wind-driven circulation. The second model, considered in the sections following, is explicitly a model of the deep circulation. Both models are severe idealizations that describe only limited aspects of the circulation.

15.5.1 Set-up of the laboratory model

Let us consider flow in a rotating tank, as illustrated in Fig. 15.10. The fluid is confined by vertical walls to occupy a sector, and the entire tank rotates anti-clockwise when viewed from above, like the Northern Hemisphere. When the fluid is stationary in the

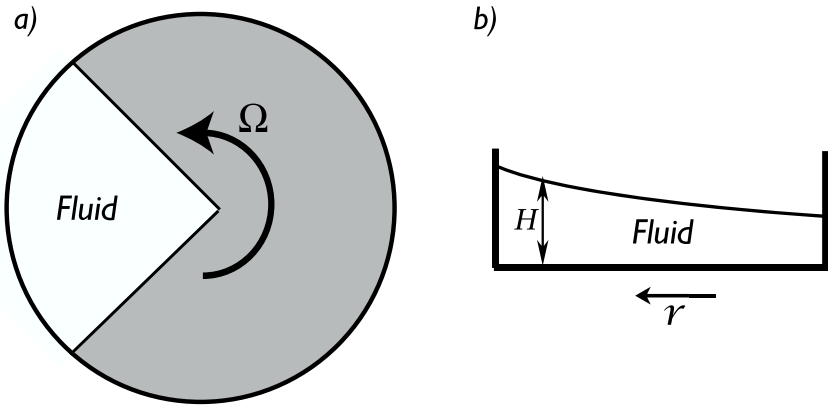

Fig. 15.10 The experimental set-up in the Stommel-Arons-Faller rotating tank experiment. (a) A plan view of the apparatus. The fluid is contained in the sector at left. (b) Side view. The free surface of the fluid slopes up with increasing radius, giving a balance (in the rotating frame) between the centrifugal force pointing outwards and the pressure force pointing inwards. Small pipes may be introduced into the fluid to provide mass sources and sinks.

rotating frame, the fluid slopes up toward the outer edge of the tank and the balance of forces in the rotating frame is between a centrifugal force pointing outwards and the pressure gradient due to the sloping fluid pointing inwards. In the inertial frame of the laboratory itself, the pressure gradient pointing inwards provides a centripetal force that causes the fluid to accelerate toward the center of the tank, resulting in a circular motion. (Recall that steady circular motion is always accompanied by an acceleration toward the center of the circle.) This set-up, and the accompanying theory, is known as the *Stommel-Arons-Faller* model.[15] The motivation of this construct is clear, in that the sector represents an ocean basin. However, rather than driving the fluid with wind or by differential heating, we drive it with localized mass sources and sinks, for example from a small pipes inserted into the tank.

15.5.2 Dynamics of flow in the tank

Let us assume that motion of the fluid in the tank is sufficiently weak that its Rossby number is small, and that it obeys the shallow water planetary geostrophic equations, namely

$$\boldsymbol{f}_0 \times \boldsymbol{u} = -g\nabla h + \Omega^2 r\,\hat{\mathbf{r}} + \boldsymbol{F}\,, \tag{15.45a}$$

$$\frac{\partial h}{\partial t} + \nabla\cdot(\boldsymbol{u}h) = S \tag{15.45b}$$

where $\hat{\mathbf{r}}$ is a unit vector in the direction of increasing r, $\boldsymbol{F}$ represents frictional terms and S represents mass sources. These two equations yield the potential vorticity equation,

$$\frac{\mathrm{D}}{\mathrm{D}t}\left(\frac{f_0}{h}\right) = \frac{\mathrm{curl}_z \boldsymbol{F}}{h} - \frac{f_0 S}{h^2}. \tag{15.46}$$

Let us write the height field as

$$h = H(r,t) + \eta(r,\theta,t) \tag{15.47}$$

where $H(r,t)$ is the height field corresponding to the rest state of the fluid (in the rotating frame) and η the perturbation. Thus, from (15.45a)

$$0 = -g\nabla H + \Omega^2 r\hat{\mathbf{r}}, \tag{15.48}$$

which gives

$$H = \frac{\Omega^2 r^2}{2g} + \hat{H}(t), \tag{15.49}$$

where $\hat{H}$ is a measure of the overall mass of the fluid. Its rate of change is determined by the mass source

$$\frac{\mathrm{d}\hat{H}}{\mathrm{d}t} = \langle S \rangle, \tag{15.50}$$

the angle brackets indicating a domain average. The equations of motion (15.45a), and (15.45b) become

$$\boldsymbol{f}_0 \times \boldsymbol{u} = -g\nabla\eta + \boldsymbol{F}, \tag{15.51a}$$

$$\frac{\partial}{\partial t}(\eta + H) + \nabla\cdot[\boldsymbol{u}(\eta + H)] = 0. \tag{15.51b}$$

Eq. (15.51a) tells us that, away from frictional regions, the velocity is in geostrophic balance with the pressure field due to the perturbation height η.

Let us now suppose $|\eta| \ll H$, which holds if the mass source is small and gentle enough. Then (15.51b) may be written

$$\frac{\partial H}{\partial t} + \nabla\cdot(\boldsymbol{u}H) = 0. \tag{15.52}$$

In this approximation, the potential vorticity equation (15.46) becomes, away from friction and mass sources,

$$\frac{\mathrm{D}}{\mathrm{D}t}\left(\frac{f_0}{H}\right) = 0 \qquad \text{or} \qquad \frac{\mathrm{D}H}{\mathrm{D}t} = 0. \tag{15.53a,b}$$

where the second equation follows because f_0 is a constant. (This equation also follows directly from (15.52), because the velocity is geostrophic and divergence-free where friction is absent; however, it is better thought of as a potential vorticity equation, not a mass conservation equation.) Eq. (15.53b) means that fluid columns change position

in order to keep the same value of H. Further, because H only varies with r, (15.53b) becomes

$$\frac{\partial H}{\partial t} + v_r \frac{\partial H}{\partial r} = 0, \tag{15.54}$$

which, using (15.49) and (15.50), gives

$$\boxed{v_r = -\frac{g}{\Omega^2 r} \langle S \rangle}. \tag{15.55}$$

This is a remarkable result, for it implies that, if $\langle S \rangle$ is positive the flow if is *toward* the apex of the dish except at the location of the mass sources and in frictional boundary layers, *no matter where the mass source is actually located*. The explanation of this counterintuitive result is simple enough: if $\langle S \rangle > 0$ the overall height of the fluid is increasing with time. Thus, in order that a given material column of fluid may keep its height fixed, it must move toward the apex of the dish. The full velocity field may be obtained, away from the frictional regions, using the divergence-free nature of the velocity:

$$\nabla \cdot \boldsymbol{u} = \frac{\partial (r v_r)}{\partial r} + \frac{\partial v_\theta}{\partial \theta} = 0. \tag{15.56}$$

Then, using (15.55), $\partial v_\theta / \partial \theta = 0$ except at a source or sink, or in a frictional boundary layer. Assuming there is only one frictional boundary layer, $v_\theta = 0$ except at those latitudes (i.e., values of r) that contain a mass source or sink.

Suppose then, that we introduce a localized mass source somewhere in the domain, and a localized mass sink of equal strength somewhere else. According to our heuristic theory, there is no flow in the interior of the domain that can provide a passage from the mass source to the sink. Thus, there must be *boundary layers* in which frictional effects are important, and which set themselves up in such a way to satisfy mass conservation. But mass conservation alone is insufficient to determine where the boundary layers might be — for this we need some vorticity dynamics. Now, away from the mass source, but including friction, the potential vorticity equation is

$$\frac{\mathrm{D}}{\mathrm{D}t}\left(\frac{f_0}{H}\right) = \frac{\mathrm{curl}_z \boldsymbol{F}}{H}, \tag{15.57}$$

and the free surface of the water slopes downward toward the apex, as illustrated in Fig. 15.10. Now, suppose that there are mass source and a sink of equal maginudes, with the source further from the apex than the sink, as in the panel at the bottom right of Fig. 15.11. The flow from source to sink must be along either the left of right boundary of the container. This flow is toward smaller values of H, and therefore the left-hand side of (15.57) is positive (just as for poleward flow in the ocean on a sphere or β-plane). To balance this the friction in the boundary current must import a positive vorticity to the flow (i.e., $\mathrm{curl}_z \boldsymbol{F} > 0$), implying a *western* boundary layer, i.e., a boundary layer on the left of the container, for then the flow itself then has an anticyclonic (clockwise) sense and friction will normally oppose this. For example, if $\boldsymbol{F} = -\lambda \boldsymbol{u}$ the right hand side of (15.57) is $-(\lambda/H)\mathrm{curl}_z \boldsymbol{u}$ and this is positive if the flow is clockwise. A little more

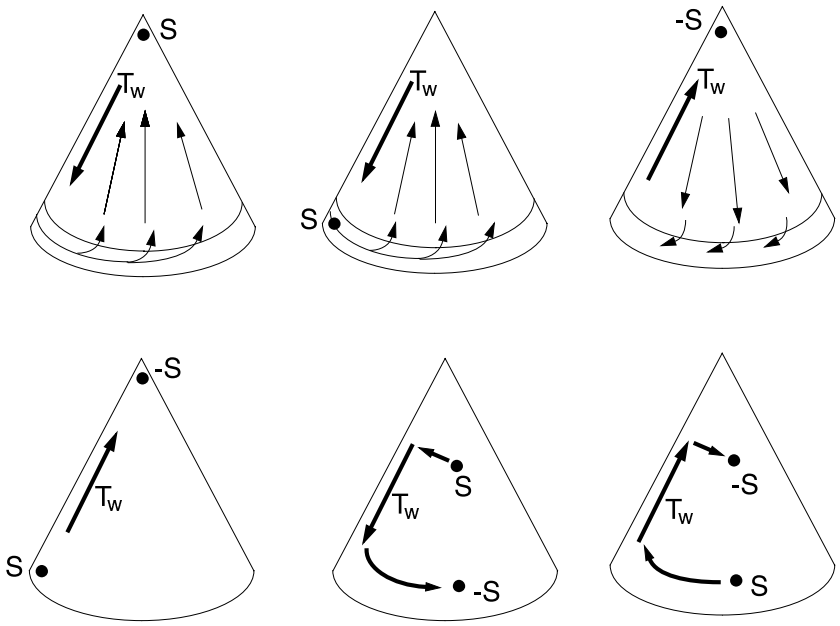

Fig. 15.11 Idealized examples of the flow in the rotating sector experiments, with various locations of a source (S) or sink ($-S$) of mass

thought will reveal that a western boundary layer is general feature of the flow, and is not dependent on the placement of mass sources or sinks. If there is only a net source of mass, as for example in the upper left example of Fig. 15.11, then the interior mass flow will be toward the apex, the flow in the boundary layer away from the apex, but again requiring a western boundary layer to achieve a balance in the potential vorticity equation. It is clear that this flow is in some ways analogous to flow on the β-plane, and that in particular:

(i) The r-dependence of the height field provides a background potential vorticity gradient, analogous to the β-effect.

(ii) The time-dependence of H is analogous to a wind curl, for it is this that ultimately drives the fluid motion.

The analogies are drawn out explicitly in shaded box on the next page; the box also includes a column for abyssal flow in the ocean, discussed in the next two sections.

15.6 A MODEL FOR OCEANIC ABYSSAL FLOW

We will now extend the reasoning applied to the rotating tank to the rotating sphere, and so construct a model — the *Stommel-Arons model* — of the abyssal flow in the ocean.[16] The basic idea is simple: we will model the deep ocean as a single layer of homogeneous fluid in which there is a localized injection of mass at high latitudes, representing convection (Fig. 15.12). However, unlike the rotating dish, mass is extracted from this layer by upwelling into the warmer waters above it, keeping the average thickness of

Analogies between a rotating dish, wind-driven and abyssal flows

Consider homogeneous models of (i) rotating dish, (ii) wind-driven flow on the β-plane, and (iii) abyssal flow on the the β-plane. We model all with a single layer of homogeneous fluid satisfying the planetary geostrophic equations. In (i) the mass source, $\langle S \rangle$, is localized and the total depth of the fluid layer changes with time; fluid columns move to keep their depth constant. In (ii) there is no mass source and depth of the fluid layer is constant; the fluid motion is determined by the wind stress curl, $\text{curl}_z \boldsymbol{\tau}$, and by β. In (iii) the fluid source (convection) is localized at high latitudes and exactly balanced by a mass loss, S_u, due to upwelling everywhere else, so that layer depth is constant and S_u is uniform and negative nearly everywhere. The equations below then apply away from frictional boundary layers and localized mass sources:

(i) Rotating dish	*(ii) Wind-driven flow*	*(iii) Abyssal flow*
PV Conservation		
$\frac{\mathrm{D}}{\mathrm{D}t}\left(\frac{f_0}{H}\right) = 0$	$\frac{\mathrm{D}}{\mathrm{D}t}\left(\frac{f}{H_0}\right) = \frac{1}{H_0}\text{curl}_z \boldsymbol{\tau}$	$\frac{\mathrm{D}}{\mathrm{D}t}\left(\frac{f}{h}\right) = -\frac{f S_u}{h^2}$
This leads to		
$v_r \frac{\partial H}{\partial r} = -\frac{\partial H}{\partial t}$	$\frac{v}{H_0}\frac{\partial f}{\partial y} = \frac{1}{H_0}\text{curl}_z \boldsymbol{\tau}$	$\frac{v}{h}\frac{\partial f}{\partial y} = -\frac{f S_u}{h^2}$
and		
$v_r = -\frac{g}{\Omega^2 r}\langle S \rangle$	$v = \frac{1}{\beta}\text{curl}_z \boldsymbol{\tau}$	$v = -\frac{f S_u h}{\beta}$
$\langle S \rangle$ is localized mass source	$\text{curl}_z \boldsymbol{\tau}$ is wind-stress curl	S_u is upwelling mass loss
Meridional mass flow away from boundaries is thus determined by:		
Sign (and not location) of localized mass source, $\langle S \rangle$.	Sign of wind-stress curl, $\text{curl}_z \boldsymbol{\tau}$.	Upwelling and sign of f, so polewards if $S_u < 0$ (upwelling).

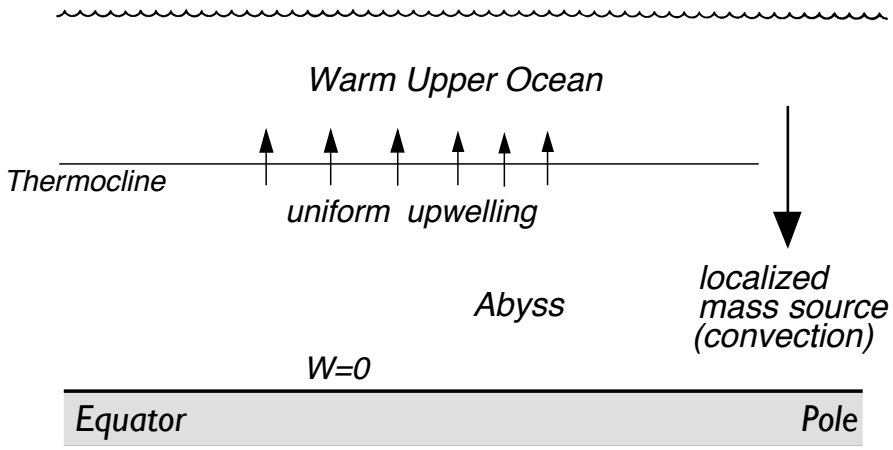

Fig. 15.12 The structure of simple Stommel-Arons ocean model of the abyssal circulation. Convection at high latitudes provides a localized mass-source to the lower layer, and upwelling through the thermocline provides a more uniform mass sink.

the abyssal layer constant. We assume that this upwelling is nearly uniform, that the ocean is flat-bottomed, and that a passive western boundary current may be invoked to satisfy mass conservation, and which does not affect the interior flow. Obviously, these assumptions are very severe and the model can at best be a conceptual model of the real ocean. Given that, we will work in Cartesian coordinates on the β-plane, and use the planetary geostrophic approximation. Our treatment in this section is physically based but quite heuristic; in section 15.7 we are a little more mathematical and a little more formal.

The momentum and mass continuity equations are

$$\boldsymbol{f} \times \boldsymbol{u} = -\nabla\phi \quad \text{and} \quad \nabla \cdot \boldsymbol{u} = -\frac{\partial w}{\partial z}, \tag{15.58}$$

which together yield the familiar balance,

$$\beta v = f\frac{\partial w}{\partial z}. \tag{15.59}$$

Except in the localized regions of convection, the vertical velocity is, by assumption, positive and uniform at the top of the lower layer, and zero at the bottom. Thus (15.59) becomes

$$v = \frac{f}{\beta}\frac{w_0}{H}. \tag{15.60}$$

where w_0 is the uniform upwelling velocity and H the layer thickness. Thus, the flow is *polewards* everywhere (including the Southern hemisphere), vanishing at the equator.

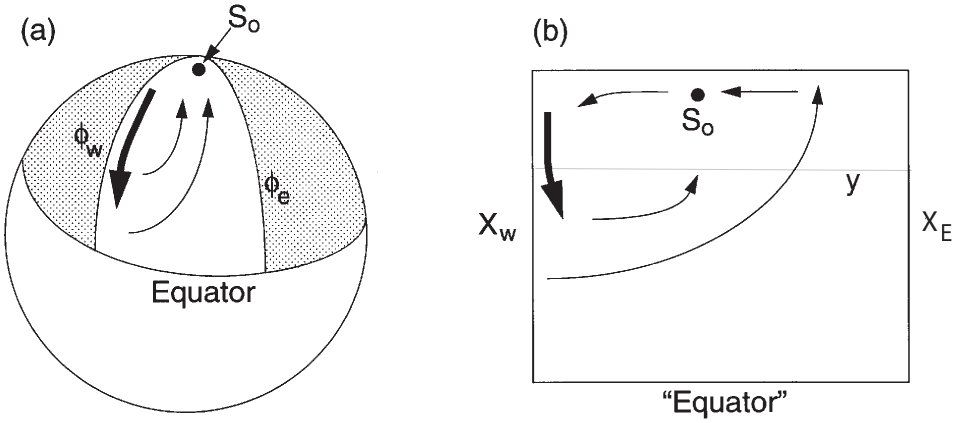

Fig. 15.13 Abyssal circulation in a spherical sector (left) and in a corresponding Cartesian rectangle (right).

15.6.1 Completing the solution

Since $v = f^{-1}(\partial\phi/\partial x)$, the pressure is given by

$$\phi = \int_{x_0}^{x} \left(\frac{f^2 w_0}{\beta H}\right) \mathrm{d}x' \tag{15.61}$$

where x_0 is a constant of integration, to be determined by the boundary conditions. Because there no flow into the Eastern boundary, x_e we set $\phi =$ constant at $x = x_e$, and because this is a one-layer model we are at liberty to set that constant equal to zero. Thus,

$$\phi(x) = -\int_{x}^{x_e} \left(\frac{f^2 w_0}{\beta H}\right) \mathrm{d}x' = -\frac{f^2}{\beta H} w_0 (x_e - x). \tag{15.62}$$

The zonal velocity follows using geostrophic balance,

$$u = \frac{1}{f}\frac{\partial\phi}{\partial y} = \frac{2}{H} w_0 (x_e - x), \tag{15.63}$$

where we have also used $\partial f/\partial y = \beta$ and $\partial\beta/\partial y = 0$. Thus the velocity is eastward in the interior, and independent of f and latitude, provided x_e is not a function of y.

Using (15.60) and (15.63) we can confirm mass conservation is indeed satisfied:

$$\frac{\partial u}{\partial x} + \frac{\partial v}{\partial y} + \frac{\partial w}{\partial z} = -\frac{2w_o}{H} + \frac{w_0}{H} + \frac{w_0}{H} = 0 \tag{15.64}$$

15.6.2 Application to the ocean

Let us consider a rectangular ocean with a mass source at the northern boundary, balanced by uniform upwelling (see figures 15.13 and 15.14). Since the interior flow will

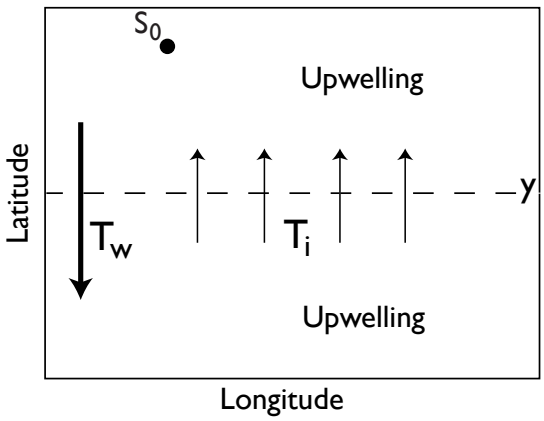

Figure 15.14 Mass budget in an idealized abyssal ocean. Polewards of some latitude y, the mass source (S_0) plus the polewards mass flux across y (T_i) are equal to sum of the southwards mass flux in the western boundary current (T_w) and the integrated loss due to upwelling (U) polewards of y. See (15.65).

be northwards, we anticipate a southwards flowing western boundary current to balance mass. Conservation of mass in the area poleward of the latitude y demands that

$$S_0 + T_i(y) = -T_w(y) + U(y) \tag{15.65}$$

where S_0 is the strength of the source, T_w the transport in the western boundary current (positive if polewards), T_i the (polewards) transport in the interior, and U is the integrated loss due to upwelling polewards of y. Then, using (15.60),

$$T_i = \int_{x_w}^{x_e} vH\,\mathrm{d}x = \int_{x_w}^{x_e} \frac{f w_o}{\beta}\,\mathrm{d}x = \frac{f}{\beta} w(x_e - x_w). \tag{15.66}$$

The upwelling loss is given by

$$U = \int_{x_w}^{x_e}\int_{y}^{y_n} w\,\mathrm{d}x = w_0(x_e - x_w)(y_n - y) \tag{15.67}$$

Assuming the source term is known, then using (15.65) we obtain the strength of the western boundary current,

$$-T_w(y) = S_0 + T_i - U = S_0 + \frac{f}{\beta} w(x_e - x_w) - w_0(x_e - x_w)(y_n - y). \tag{15.68}$$

To close the problem we note that over the entire basin mass must be balanced, which gives a relationship between w and S_0,

$$S_0 = w_0 \Delta x \Delta y, \tag{15.69}$$

where $\Delta x = x_e - x_w$ and $\Delta y = y_n - y_s$. where y_s is the southern boundary of the domain. Using (15.69), (15.68) becomes

$$\begin{aligned} -T_w(y) &= -w_0\left(\Delta x(y_n - y) - \frac{f}{\beta}\Delta x - \Delta x \Delta y\right) \\ &= w_0 \Delta x\left(y - y_s + \frac{f}{\beta}\right). \end{aligned} \tag{15.70}$$

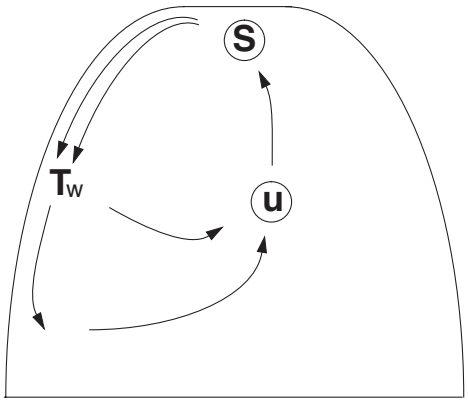

Figure 15.15 Schematic of a Stommel-Arons circulation in a single sector. The transport of Western boundary current is greater than that provided by the source at the apex, illustrating the property of *re-circulation.* The transport in the western boundary current T_w decreases in intensity equatorwards, as it loses mass to the polewards interior flow, and thence to upwelling. The integrated sink, due to upwelling, U, exactly matches the strength of the source, S.

With no loss of generality we will take $y_s = 0$ and $f = f_0 + \beta y$. Then (15.70) becomes

$$-T_w(y) = w_0 \Delta x \, (2y + f_0/\beta) \tag{15.71}$$

or, using $S_0 = w_0 \Delta x y_n$,

$$-T_w(y) = \frac{S_0}{y_n}\left(2y - \frac{f_0}{\beta}\right). \tag{15.72}$$

With a slight loss of generality (but consistent with the spirit of the planetary geostrophic approximation) we take $f_0 = 0$, which is equivalent to supposing that the equatorial boundary of the domain is at the equator, and finally obtain

$$\boxed{T_w(y) = -2S_0 \frac{y}{y_n}.} \tag{15.73}$$

At the northern boundary this becomes

$$T_w(y) = -2S_0, \tag{15.74}$$

which means that the flow southwards from the source is twice the strength of the source itself. We also see that:

(i) The western boundary current is equatorwards everywhere;

(ii) At the northern boundary the equatorwards transport in the western boundary current is equal to *twice* the strength of the source;

(iii) The northwards mass flux at the northern boundary is equal to the strength of the source itself.

We may check this last point directly: from(15.66)

$$T_I(y_n) = \frac{\beta y_n}{\beta} w_0 \Delta x = S. \tag{15.75}$$

The fact that convergence at the 'pole' balances T_w and S_0 does not of course depend on the particular choice we made for f and y_s.

The flow pattern evidently has the property of *recirculation* (see Fig. 15.15): this is one of the most important properties of the solution, and one that is likely to transcend all the limitations inherent in the model. This single-hemisphere model may be thought of as a crude model for aspects of the abyssal circulation in the North Atlantic, in which convection at high latitudes near Greenland is at least partially associated with the abyssal circulation. In the North Pacific there is, in contrast, little if any deep convection to act as a mass source. Rather, the deep circulation is driven by mass sources in the opposite hemisphere, and we now consider a simple model of this.

15.6.3 A two hemisphere model

Our treatment now is even more obviously heuristic, since our domain crosses the equator yet we continue to use the planetary geostrophic equations, invalid at the equator. We also persist with Cartesian geometry, even for these global-scale flows. In our defense, we note that the value of the solutions lies in their qualitative structure, not in their quantitative predictions. Let us consider a situation with a source in the Southern Hemisphere but none in the Northern Hemisphere. For later convenience we take the Southern Hemisphere source to be of strength $2S_0$, and we suppose the two hemispheres have equal area. As before, the upwelling is uniform, so that to satisfy global mass balance

$$S_0 = w_0 \Delta x \Delta y \tag{15.76}$$

where $\Delta x \Delta y$ is the area of each hemisphere. Then, given w_0, the zonally integrated polewards interior flow in each hemisphere, away from the equator, follows from Sverdrup balance,

$$T_i(y) = \frac{f}{\beta} w_0 (x_e - x_w) = S_0 \frac{y}{y_p} \tag{15.77}$$

where y_p is either y_n (the northern boundary) or y_s. The western boundary current is assumed to 'take up the slack,' that is to be able to adjust its strength to satisfy mass conservation. Thus, since $T_i(y_n) = S_0$, where S_0 is half the strength of the source in the *southern* hemisphere, it is plain that there must be a southwards flowing western boundary current near the northern end of the northern hemisphere, even in the absence of any deep water formation there!

In the northern hemisphere, the total loss due to upwelling polewards of a latitude y is given by

$$U(y) = w_0 \Delta x |y_n - y| \tag{15.78}$$

The strength of the western boundary current is then given by

$$T_w(y) = U - T_i = w_0 \Delta x (y_n - y) - \frac{f}{\beta} w_0 \Delta x = w_0 \Delta x (y_n - 2y) \tag{15.79}$$

using $f = \beta y$. Thus, at $y - y_n$,

$$T_w(y_n) = -w_0 \Delta x y = -S. \tag{15.80}$$

The boundary current changes sign halfway between equator and pole, at $y = y_n/2$. (In

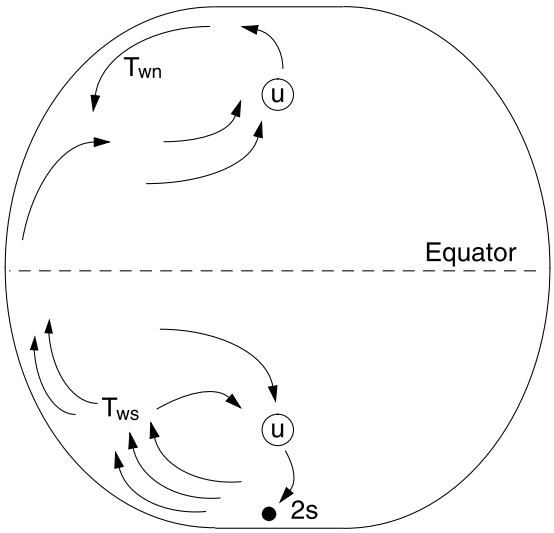

Figure 15.16 Schematic of a Stommel-Arons circulation in a two-hemisphere basin. There is only one mass source, and this is in the Southern hemisphere and for convenience it has a strength of 2. Although there is no source in the Northern Hemisphere, there is still a western boundary current and a recirculation. The integrated sinks due to upwelling exactly match the strength of the source.

spherical coordinates, the analogous critical latitude turns out to be at $\theta = \sin^{-1}(1/2)$.) The solution is illustrated schematically in Fig. 15.16. We can (rather fancifully) imagine this to represent the abyssal circulation in the Pacific Ocean, with no source of deep water at high northern latitudes.

15.7 * A SHALLOW WATER MODEL OF THE ABYSSAL FLOW

We can obtain a more complete solution of the flow that explicitly includes the western boundary current by constructing a shallow water Stommel-Arons type model of the abyssal circulation.[17] However, the essential dynamics is the same as that of the previous section. The model is similar to that illustrated in Fig. 15.12 and comprises a single moving layer of homogeneous fluid lying underneath a lighter, stationary layer. The lower fluid is forced by a mass source at its polewards end that represents convection, and by a uniform mass sink everywhere else that represents diffusive upwelling into the upper layer. The mass source and sink are specified — that is, they are not functions of the flow — and are equal and opposite, so that there is no net mass source. The motion of the lower layer is then governed by the planetary geostrophic reduced-gravity shallow water equations (sections 3.2 and 5.2), to wit:

$$-fv = -g'\frac{\partial h}{\partial x} - ru, \qquad fu = -g'\frac{\partial h}{\partial y} - rv, \tag{15.81a}$$

$$\frac{\partial h}{\partial t} + \nabla \cdot (\boldsymbol{u}h) = S, \tag{15.81b}$$

Here h is the thickness of the lower layer (below the thermocline of Fig. 15.12), g' is the reduced gravity between the two layers, and r is a constant frictional coefficient; we will assume this is small, and in particular that $r \ll f$. The mass source term S on the right-hand side of the mass continuity equation represents both upwelling and

a localized convective source at the polewards end of the domain. We will suppose the upwelling is uniform and that, when integrated over area, it exactly balances the convective mass source. Thus, we write $S = S_0 + S_u$ where S_u is uniform and negative, S_0 is the localized convective source, and $\int_A S \, \mathrm{d}A = 0$.

15.7.1 Potential vorticity and polewards interior flow

Straightforward manipulation of (15.81) gives the potential vorticity equation

$$\frac{\mathrm{D}}{\mathrm{D}t}\left(\frac{f}{h}\right) = -\frac{r}{h}\mathrm{curl}_z \boldsymbol{u} - \frac{fS_u}{h^2}. \tag{15.82}$$

Away from boundaries the first term on the right-hand side is negligible, and so, away from the convective source and in a steady state (15.82) becomes

$$\frac{\beta v}{h} + \frac{f}{h^2}\boldsymbol{u}\cdot\nabla h = -\frac{fS_u}{h^2}. \tag{15.83}$$

However, the second term on the left-hand side is small if friction is small, for then the flow is nearly in geostrophic balance and, using (15.81a) with $r = 0$, it follows that

$$f\boldsymbol{u}\cdot\nabla h = -g'\frac{\partial h}{\partial y}\frac{\partial h}{\partial x} + g'\frac{\partial h}{\partial x}\frac{\partial h}{\partial y} = 0. \tag{15.84}$$

The potential vorticity equation is then just

$$\beta v = -fS_u/h, \tag{15.85}$$

and because $S_u < 0$ the flow is polewards, regardless of the location of the convective mass source. From the perspective of the continuously stratified equations, the corresponding potential vorticity equation is just

$$\beta v = f\frac{\partial w}{\partial z} \tag{15.86}$$

Upwelling from the abyss into the upper ocean corresponds to a postive value of the stretching term $f\partial w/\partial z$, and again the interior flow is polewards.

15.7.2 The solution

It is convenient to deal with mass transports rather than velocities and we define $\boldsymbol{U} \equiv U\mathbf{i} + V\mathbf{j} \equiv uh\mathbf{i} + vh\mathbf{j}$. Away from the convective source equations of motion, (15.81), become, in steady state,

$$-fV = -\frac{\partial \Phi}{\partial x} - rU, \qquad fU = -\frac{\partial \Phi}{\partial y} - rV, \tag{15.87a}$$

$$\nabla\cdot\boldsymbol{U} = S_u, \tag{15.87b}$$

where $\Phi = g'h^2/2$. For small friction ($r \ll f$) we may write (15.87a) as

$$V = \frac{1}{f}\frac{\partial \Phi}{\partial x} - \frac{r}{f^2}\frac{\partial \Phi}{\partial y}, \qquad U = -\frac{1}{f}\frac{\partial \Phi}{\partial y} - \frac{r}{f^2}\frac{\partial \Phi}{\partial x}, \tag{15.88a,b}$$

which, after differentiation and use of (15.87b), combine to give

$$\frac{\beta}{f}\frac{\partial \Phi}{\partial x} = -fS_u - f\nabla\cdot\left(\frac{r}{f^2}\nabla\Phi\right). \tag{15.89}$$

In the interior where the effects of friction are small (15.89) becomes $\beta V = -fS$, so recovering (15.85) and imlying polewards interior flow. However, by mass conservation, the flow cannot be polewards at all longitudes, for reasons similar to those articulated in section 14.1.1 we expect there to be a frictional western boundary current. We thus let $\Phi = \Phi_I + \Phi_b$, where Φ_I is the interior field and Φ_b the boundary layer correction. The interior field obeys $\partial\Phi_I/\partial x = -(f^2/\beta)S$ and therefore given by, for constant S,

$$\Phi_I(x, y) = \frac{f^2}{\beta}S_u(x_e - x) + \Phi_e \tag{15.90}$$

where Φ_e is the value of Φ_I at the eastern boundary, x_e. This does not affect the solution and may be set to zero.

In the western boundary layer the the dominant balance in (15.89) is

$$\beta\frac{\partial \Phi_b}{\partial x} = -r\frac{\partial^2 \Phi_b}{\partial x^2}, \tag{15.91}$$

with solution

$$\Phi_b = P(y)\exp(-\beta x/r), \tag{15.92}$$

where $P(y)$ is to be determined by mass conservation: the southwards mass flux at a latitude y in the western boundary current must be equal to the sum of the polewards mass flux in the interior at that latitude, plus the total mass lost to upwelling equatorwards of y (see Fig. 15.14). These fluxes are:

$$\text{Upwelling flux} = \int_0^{x_e}\int_0^{y} S_u\,\mathrm{d}x\,\mathrm{d}y = S_u x_e y, \tag{15.93}$$

using the definition of S;

$$\text{Interior flux} = \int_0^{x_e} V\,\mathrm{d}x = \frac{1}{f}\int_0^{x_e}\frac{\partial \Phi_I}{\partial x}\,\mathrm{d}x = \frac{1}{f}[\Phi_e - \Phi_I(0, y)] = -\frac{f}{\beta}Sx_e, \tag{15.94}$$

using (15.90); and

$$\text{Boundary flux} = \int_0^{\infty}\frac{1}{f}\frac{\partial \Phi_b}{\partial x}\,\mathrm{d}x = P(y), \tag{15.95}$$

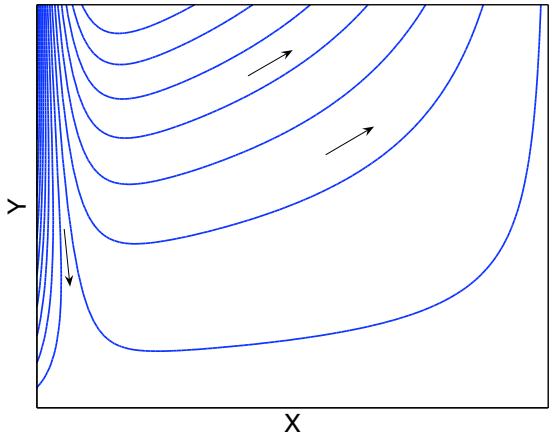

Figure 15.17 The pressure field Φ for the shallow-water Stommel-Arons model, as given by (15.98) with $r/\beta = 0.04x_e$, $f = \beta y$, and $y = 0$ at the equatorwards edge of the domain. The arrows indicate the flow direction, with the western boundary current diminishing in intensity as it moves equatorwards. The convective mass source is, implicitly, just polewards of the domain. (Note that the pressure field is not exactly a streamline.)

using (15.88a), neglecting the very small term $r\partial\Phi/\partial y$, and (15.92). By mass conservation we have

$$P(y) = S_u x_e y + \frac{f}{\beta} S_u x_e, \tag{15.96}$$

and if $f = \beta y$ and the domain goes from $y = 0$ to $y = y_n$ this becomes

$$P(y) = 2S_u x_e y = -2S_0 \frac{y}{y_n}, \tag{15.97}$$

where the second equality follows because the integrated upwelling balances the mass source. Consistent with our earlier heuristic treatment, the western boundary curren: there

(i) is equatorwards, away from the convective mass source;
(ii) diminishes in intensity as it moves equatorwards, as it feeds the interior;
(iii) has a maximum mass flux of twice that of the convective source; that is, the flow recirculates.

Using (15.90) and (15.97) the complete (western boundary layer plus interior) solution is thus given by

$$\Phi = \Phi_I + \Phi_b = \frac{f^2}{\beta} S_u (x_e - x) + 2S_u x_e y e^{-\beta x/r}, \tag{15.98}$$

and this is plotted in Fig. 15.17. This solution does not, of course, include the flow in the neighbourhood of the convective source itself, nor does it satisfy no-normal flow conditions at the polewards edge of the domain.

15.8 SCALING FOR THE BUOYANCY-DRIVEN CIRCULATION

Thus far, we have taken the strength of the upwelling as a given. In reality, this is a consequence of the presence diapycnal diffusion, because in its absence the flow is along isopycnals. In section 15.2 we estimated the upwelling for a non-rotating model;

we now do the same for a fluid obeying the steady planetary geostrophic equations, namely

$$\boldsymbol{v} \cdot \nabla b = \kappa \nabla^2 b, \qquad \nabla \cdot \boldsymbol{u} + \frac{\partial w}{\partial z} = 0 \tag{15.99a,b}$$

$$\boldsymbol{f} \times \boldsymbol{u} = -\nabla \phi, \qquad b = \frac{\partial \phi}{\partial z}. \tag{15.100a,b}$$

On the first line we have the thermodynamic equation and the mass continuity equation, and on the second line we have the momentum equations, that is geostrophic and hydrostatic balance, respectively. We use the continuously stratified equations rather than the corresponding shallow water equations because the former allow for a straightforward representation of diapycnal diffusion.

The momentum and mass continuity equations combine to give the linear geostrophic vorticity equation and the thermal wind equation and associated scales as follows:

$$\beta v = f \frac{\partial w}{\partial z} \quad \rightarrow \quad \beta U = \frac{f_0 W}{\delta}, \tag{15.101a}$$

$$f \frac{\partial \boldsymbol{u}}{\partial z} = \mathbf{k} \times \nabla b \quad \rightarrow \quad f \frac{U}{\delta} = \frac{\Delta b}{L}. \tag{15.101b}$$

We use uppercase to denote scaling variables, except that the vertical scale is denoted δ and the scaling for buoyancy variations is denoted Δb. We will take Δb is given, and equal to the buoyancy difference at the surface that is ultimately driving the motion. We also assume that the horizontal scales are isotropic, with $U = V$ and $X = Y = L$. The thermodynamic relation gives a relationship between W, κ and δ if we assume a broad upwelling region with a balance between upwards advection and diffusion:

$$w \frac{\partial b}{\partial z} = \kappa \frac{\partial^2 b}{\partial z^2} \quad \rightarrow \quad W = \frac{\kappa}{\delta}. \tag{15.102}$$

Eliminating U from (15.101) gives

$$W = \frac{\delta^2 \beta \, \Delta b}{f^2 L}. \tag{15.103}$$

and using this with (15.102) gives scalings for the vertical velocity and δ:

$$\boxed{W = \kappa^{2/3} \left(\frac{\beta \, \Delta b}{f^2 L} \right)^{1/3} \qquad \delta = \kappa^{1/3} \left(\frac{f^2 L}{\beta \, \Delta b} \right)^{1/3}}. \tag{15.104a,b}$$

These scalings mean that (in so far as (15.100) describes the flow) the upwelling strength, and the circulation more generally, are dependent on a finite value of the diffusivity, and scale as the $2/3$ power of that diffusivity. The upwelling water is cold but the water at the surface is warm, and (15.104b) is a measure of the depth of the transition region — that is, the thickness of the thermocline, a topic we return to in more detail in the next chapter. We will make one important point now though: In order for the scales given in (15.104) to be at all representative of those observed in the real ocean, we must use

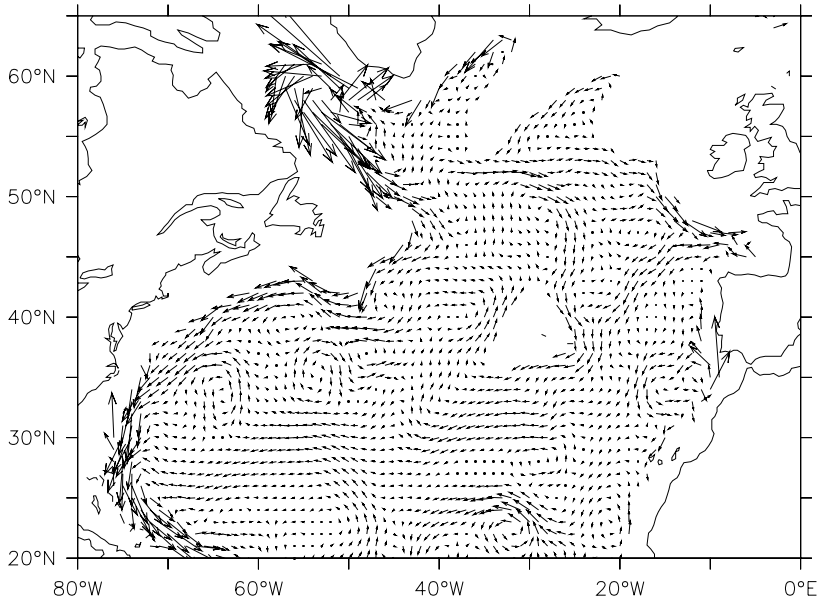

Fig. 15.18 The ocean currents at a depth of 2500 m in the North Atlantic, obtained using a combination of observations and model (as in Fig. 14.2). Note the southwards flowing *deep western boundary current*.

an eddy diffusivity for κ. Using $f = 10^{-4}\,\mathrm{s}^{-1}$, $\beta = 10^{-11}\,\mathrm{m}^{-1}\,\mathrm{s}^{-1}$, $L = 5 \times 10^6\,\mathrm{m}$, $g = 10\,\mathrm{m\,s}^{-2}$, $\kappa = 10^{-5}\,\mathrm{m}^2\,\mathrm{s}^{-1}$, $\Delta b = -g\Delta\rho/\rho_0 = g\beta_T \Delta T$ and $\Delta T = 10\,\mathrm{K}$ we find $\delta \approx 150\,\mathrm{m}$ and $W = 10^{-7}\,\mathrm{m\,s}^{-1}$, not unreasonable values albeit δ is rather smaller than the thickness of the observed thermocline. However, if we take the molecular value of $\kappa \approx 10^{-7}\,\mathrm{m}^2$ the values of W and δ are much smaller, and unrealistically so. Evidently, if the deep circulation of the ocean is buoyancy driven, it must take advantage of turbulence that enhances the small scale mixing and produces an eddy diffusivity.

15.8.1 Summary remarks on the Stommel-Arons model

If we were given the location and strength of the sources of deep water in the real ocean, the Stommel-Arons model could give us a global solution for the abyssal circulation. The solution for the Atlantic, for example, resembles a superposition of Fig. 15.15 and Fig. 15.16 (with deep water sources in the Weddell Sea and near Greenland), and that for the Pacific resembles Fig. 15.16 (with a deep water source emanating from the Antarctic Circumpolar Current). Perhaps the greatest success of the model is that it introduces the notions of deep western boundary currents and recirculation — enduring concepts of the deep circulation that remain with us today. For example, the North Atlantic does have a well-defined deep western boundary current running south along the Eastern seaboard of Canada and the United States, as seen in Fig. 15.18.[18] However, in other important aspects the model is found to be in error, in particular it is found that there is little upwelling through the main thermocline — much of the water formed by

deep convection in the North Atlantic in fact upwells in the Southern Hemisphere.[19] Are there fundamental problems with the model, or just discrepancies in details that might be corrected with a slight reformulation? To help answer that we summarize the assumptions and corresponding predictions of the model, and distinguish the essential aspects from what is merely convenient.

(i) A foundational assumption is that of linear geostrophic vorticity balance in the ocean abyss, represented by $\beta v \approx f \partial w/\partial z$, or its shallow water analog.

— The effects of mesoscale eddies are thereby neglected. As discussed in chapter 9, in their mature phase mesoscale eddies seek to barotropize the flow, and so create deep eddying motion that might dominate the deep flow.

(ii) A second important assumption is that of uniform upwelling, across isopycnals, into the upper ocean, and that $w = 0$ at the ocean bottom. When combined with (i) this gives rise to polewards interior flow, and by masss conservation a deep western boundary current. The upwelling is a consequence of a finite diffusion, which in turn leads to deep convection as in the model of sideways convection of section 15.2.

— The uniform-upwelling assumption might be partially relaxed, while remaining within the Stommel-Arons framework, by supposing (for example) that the upwelling occurs near boundaries, or intermittently, with corresponding detailed changes to the interior flow.

— If bottom topography is important, then $w \neq 0$ at the ocean bottom. This effect may be most important if mesoscale eddies are present, for then in an attempt to maintain its value of potential vorticity the abyssal flow will have a tendency to meander nearly inviscidly along contours of constant topography. In the presence of a mid-ocean ridge, some of the deep western boundary current might travel meridionally along the eastern edge of the ridge instead of along the coast.

— The deep water may not upwell across isopycnals at at all, but may move along isopycnals that intersect the surface (or are connected to the surface by convection). If so, then in the presence of mechanical forcing a deep circulation could be maintained even in the absence of a diapycnal diffusivity. The circulation might then be qualitatively different from the Stommel-Arons model, although a linear vorticity balance might still hold, with deep western boundary currents. This is discussed in section 16.5.

Note that, even if Stommel-Arons picture were to be essentially correct, we should not consider the deep flow is being driven by deep convection at the source regions. It is a *convenience* to specify the strength of these regions for the calculations but, just as in the models of sideways convection considerer in section 15.2, the overall strength of the circulation (insofar as it is thermally driven) is a function of the size of the diffusivity and the meridional temperature gradient at the surface.

Notes

1 See, for example, Warren (1981) who provides a review and historical background and Schmitz (1995) who surveys the observations and provides an interpretation of the deep global circulation.

2 From Wunsch (2002).

3 Courtesy of L. Talley

4 Adapted from Paparella and Young (2002).

5 As in Haney (1971). Only the value of C, and not the value of κ, is material to the boundary condition written in this form, because we are parameterizing only the flux at the surface. The parameter C is often taken to be such that the heat flux is of order $30\,\mathrm{W\,m^{-2}\,K^{-1}}$, but it is not a universal constant.

6 Rossby (1965).

7 Adapted from Rossby (1998).

8 Ocean convection is reviewed by Marshall and Schott (1999).

9 I am grateful to W. R. Young for some useful comments on this.

10 Sandström (1908, 1916). However, Sandström did not prove the result encapsulated by (15.23); his discussion was thermodynamic, in terms of a Carnot cycle, and the dissipation of kinetic energy played no role in his argument. Since that time various related statements with varying degrees of generality and preciseness have been given (see e.g., Huang 1999). The more rigorous result (15.23) is a statement about a kinetic-energy dissipating circulation, and it does not prove that unless the heating occurs at a lower level than the height then no circulation at all can be maintained.

11 Following Paparella and Young (2002).

12 The original box model is due to Stommel (1961), and many studies with variations around this have followed. Rooth (1982) developed the idea of a buoyancy-driven pole-to-pole overturning circulation, and Welander (1986) discussed, among other things, the role of boundary conditions on temperature and salinity at the ocean surface. Thual and McWilliams (1992) systematically explored how box models compare with two-dimensional fluid models of sideways convection, Quon and Ghil (1992) explored how multiple equilibria arise in related fluid models, and Dewar and Huang (1995) discussed the problem of flow in loops. Cessi and Young (1992) tried to derive simple models systematically from the equations of motion, obtaining various nonlinear amplitude equations. Our discussion is of just a fraction of all this; see also Whitehead (1995), Cessi (2001) and Dijkstra (2002) for reviews and more discussion.

13 Adapted from Welander (1986) and Dijkstra (2002).

14 Bryan (1986), Manabe and Stouffer (1988) and Marotzke (1989) did find evidence of multiple equilibria in various three-dimensional numerical models.

15 After Stommel et al. (1958).

16 Following Stommel and Arons (1960).

17 Motivated by Cessi (2001).

18 A global Stommel-Arons-like solution was presented by Stommel (1958). The dis-

covery of deep western boundary currents, by Swallow and Worthington (1961), was motivated by the theoretical model. Using neutrally-buoyant floats underneath the Gulf Stream they found a robust equatorwards-flowing undercurrent with typical speeds of 9–$18\,\mathrm{m\,s^{-1}}$. Relevant observations of the deep circulation are summarized by Hogg (2001).

19 For example, Toggweiler and Samuels (1995).

Problems

15.1 *(a)* Obtain an expression analogous to (15.23) for the anelastic equations.
(b) ♦ Obtain, if possible, an expression analogous to (15.23) for a compressible gas (which you may suppose to be ideal, if needed). Interpret the result.

15.2 ♦ Consider a model of sideways convection in which the boundary condition at the top is the relaxation, or Haney, condition $b_z = A(b^*(y) - b)$ where A (a constant) and $b^*(y)$ are given, b is the buoyancy, proportional to the temperature, the other boundaries are insulating, and the flow is statistically steady.

(a) Is it still the case that on average the fluid is heated (i.e., there is a heat flux into the fluid through the upper surface) where it is already warm? If so, how may this be reconciled with the intuition that if the ocean surface is anomalously warm it will cool by way of a heat flux from the ocean to the atmosphere?
(b) Show that if $A < 0$ a statistically steady state cannot be reached.
(c) Suppose that b^* varies monotonically with latitude. Show that if κ is non-zero, the average surface temperature gradient will be less than that of b^*.

15.3 Consider a variation of the Stommel box model in which the equation of motion (15.35) is replaced by

$$\frac{\mathrm{d}T}{\mathrm{d}\tau} = (1-T) - \Phi^2 T, \quad \frac{\mathrm{d}S}{\mathrm{d}\tau} = \delta(1-S) - \Phi^2 S, \quad \Phi = -\gamma(T - \mu S). \qquad \text{(P15.1)}$$

The interbox flow equations now depends on the density difference squared, so allowing continuous equations. Show that multiple equilibria are possible, and that one is thermally driven and one salinity driven. Obtain approximate expressions for the temperature and salinity for these equilibria, in the limit of large γ and small δ if you wish. If δ is large, what changes about these solutions?

15.4 *(a)* In the Stommel two-box problem, show physically that when three solutions are present, the middle one is generally unstable. One way to do this is to suppose that the system is perturbed slightly from that equilibrium, and argue qualitatively that the forces on the system will then take it farther from that state. By use of similar arguments, show that the other solutions are generally stable.
(b) ♦ Alternatively, linearize the equations about the equilibrium points and show that small perturbations will grow if the solution is that of the middle equilibrium state, but will be damped in the other two cases.

15.5 ♦ Obtain the solution to (15.16) at lowest order. Take the solution to higher order and show that the sinking region is narrower than the upwelling region.